Lehrstuhl für Energieverbundtechnik

Head of Department

Univ.-Prof. Dipl.-Ing. Dr.techn. Thomas Kienberger

Franz-Josef-Straße 18, A-8700 Leoben

Website: evt.unileoben.ac.at

Simulation and operational modes of a plug and play storage for photovoltaic power

Master Thesis

created at the

Lehrstuhl für Energieverbundtechnik

Author:

Alejandra Kollros

11742833

Supervisors:

Univ.-Prof. Dipl.-Ing. Dr.techn. Thomas Kienberger

Dipl.-Ing. Dr.mont. Andreas Hammer

Dipl.-Ing. Benjamin Böckl

Leoben, September 2018

Affidavit

I declare in lieu of oath, that I wrote this thesis and performed the associated research myself, using only literature cited in this volume.

Signature | Place, Date

Eidesstattliche Erklärung

Ich erkläre an Eides statt, dass ich diese Arbeit selbstständig verfasst, andere als die angegebenen Quellen und Hilfsmittel nicht benutzt und mich auch sonst keiner unerlaubten Hilfsmittel bedient habe.

Unterschrift | Ort, Datum

Abstract

Renewable energy has become an important topic of today's world. Renewable energy resources are inexhaustible, clean and they can be used in a decentralized way, i.e they can be generated and consumed directly in the same place, for example in domestic applications. In the last decades, the share of renewable energy in the energy mix has increased considerably, mainly because of the strict legislations and policies involving climate and energy goals and targets, but also without question, the increased self awareness and public perception regarding climate change and energy savings, in the citizens and as well in businesses or industries, therefore supporting the transition to a decarbonized energy system. However, since renewable energy often relies on weather conditions for the generation of power (e.g. in photovoltaic (PV) systems during the nighttime or during cloudy days where there is none or little energy production), problems such as unpredictability and unreliability emerge. Therefore, energy storage systems play an important role in creating a flexible and reliable system. In this work, a model of a complete domestic PV-battery system is modeled and simulated, whose goal is to develop a realistic model of a Plug & Play Storage of Photovoltaic Power (P^3P), a product that is currently being made by a start-up company in Graz. Said model firstly includes a PV module modeled in Simulink which also includes an irradiance model that relies in real measured data. Secondly, a battery model has been implemented in MATLAB by means of power and energy balances, with one control strategy which also includes four different operational modes and additionally aging effects have been implemented. Thirdly, based on real data and by means of curve fitting, an inverter model has also been developed in MATLAB. The special feature of the aforementioned system is that energy can be purchased from the grid but the surplus of generated energy cannot be fed into it. Finally, a sensitivity analysis was carried out to quantify and evaluate the influence of changing the predefined standard parameters over the whole system by comparing it to a performance parameter, enabling to find the best system configuration for the considered scenario.

Kurzfassung

Erneuerbare Energie ist zu einem wichtigen Thema der heutigen Welt geworden. Erneuerbare Energiequellen sind unerschöpflich, sauber und können dezentral genutzt werden, das heißt Sie können direkt am selben Ort erzeugt und verbraucht werden, beispielsweise in häuslichen Anwendungen. In den letzten Jahrzehnten hat der Anteil erneuerbarer Energien am Energiemix erheblich zugenommen, vor allem aufgrund der strengen Gesetzgebung und Politik mit Klima - und Energiezielen, aber auch dem gestiegenen Selbstbewusstsein und der öffentlichen Wahrnehmung in Bezug auf den Klimawandel und Energieeinsparungen, sowohl Bürger als auch in Unternehmen oder Industriezweigen, unterstützen daher den Übergang zu einem dekarbonisierten Energiesystem. Da erneuerbare Energie jedoch oft auf Wetterbedingungen für die Erzeugung von Energie angewiesen ist (zum Beispiel in Photovoltaik (PV) -Systemen während der Nacht oder an bewölkten Tagen, an denen es keine oder nur wenig Energieproduktion gibt), treten Probleme wie Unvorhersehbarkeit und Unzuverlässigkeit auf. Daher spielen Energiespeichersysteme eine wichtige Rolle bei der Schaffung eines flexiblen und zuverlässigen Systems. In dieser Arbeit wird ein Modell eines kompletten häuslichen PV-Batteriesystems erstellt und simuliert, dessen Ziel es ist, ein realistisches Modell eines Plug & Play Storage of Photovoltaic Power (P^3P) zu entwickeln, ein Produkt, das wird derzeit von einem Start-up-Unternehmen in Graz hergestellt. Dieses Modell enthält zunächst ein in Simulink modelliertes PV-Modul, das auch ein Strahlungsmodell enthält, das auf realen Messdaten beruht. Zweitens wurde ein Batteriemodell in MATLAB mit Hilfe von Leistungs- und Energiebilanzen implementiert. Diese Implementierung enthält eine Regelungsstrategie welche vier verschiedene Betriebsmodi sowie Alterungseffekte umfasst. Drittens, basierend auf realen Daten und mittels Kurvenanpassung, wurde auch ein Wechselrichtermodell in MATLAB entwickelt. Die Besonderheit der vorgenannten System besteht darin, dass Energie aus dem Netz bezogen werden kann, der Überschuss an erzeugter Energie jedoch nicht zurück in das Netz eingespeist werden kann. Schließlich wurde eine Sensitivitätsanalyse durchgeführt, um den Einfluss der Änderung der vordefinierten Standardparameter auf das Gesamtsystem zu quantifizieren und zu bewerten, indem diese mit einem Leistungsparameter verglichen werden, um die beste Systemkonfiguration für das betrachtete Szenario zu finden.

Contents

List of Figures

List of Tables

Abbreviations and Nomenclature

Abbreviations

CO_2 Carbon dioxide

P^3P Plug & Play Storage of Photovoltaic Power

a-Si Amorphous Silicon

AC Alternating Current

BIPV Building Integrated Photovoltaics

c.f. Refer to

CHP Combined Heat and Power

CIGS Copper Indium Gallium Selenide

CLR Curtailment Loss Ratio

DC Direct Current

DOD Depth of Discharge

DSO Distribution System Operator

DSS Degree of Self-sufficiency

EES Energy Storage System

ES Energy Storage

EU European Union

EV Electric vehicle

GHG Greenhouse Gas

HEV Hybrid Electric vehicle

IGTB Insulated Gate Bipolar Transistor

LA Lead-Acid

LIB Lithium-ion Batteries

mc-Si Multicrystalline Silicon

MOSFET Metal Oxide Field Effect Transistors

MPP Maximum Power Point

MPPT Maximum Power Point Tracking

OPC Organic Photovoltaic Cells

PV Photovoltaic

SCR Self-consumption Rate

SMES Superconducting Magnetic Energy Storage

SOC State of Charge

SOH State of Health

TPFV Thin-film photovoltaic

TSO Transmission System Operator

Nomenclature

β	Surface's inclination
δ	Brightness parameter
ϵ	Clearness parameter
γ	Surface's orientation
ω	Hour angle
ϕ	Latitude
ρ_{g}	Ground reflection
θ	Angle of incidence
θ_{z}	Zenith angle
A	Ideality factor
a	Modified ideality factor
G	Irradiation on the photovoltaic's surface
G_{n}	Nominal irradiation
G_{sc}	Solar constant
I	Output current
I_0	Reverse saturation or leakage current of the diode
$I_{\mathrm{b,n}}$	Normal incidence beam radiation
I_{b}	Beam radiation
I_{d}	Diode current

I_{on}	Extraterrestrial normal incidence radiation
I_{o}	Extraterrestrial radiation
I_{ph}	Photogenerated current
$I_{d,T}$	Diffuse radiation on a tilted collector
k	Boltzmann constant
k_{T}	Clearness index
m	Air mass
N_{s}	Number of PV cells connected in series
q	Electron constant
R_p	Equivalent parallel resistance of the photovoltaic module
R_s	Equivalent series resistance of the photovoltaic module
T_{c}	Cell temperature
V	Output voltage
V_{T}	Thermal voltage
n	Day of the year
x	Hour of the year

1. Introduction

Nowadays, topics such as renewable energy or energy efficiency have gained significant importance, due to the world becoming increasingly concerned about its energy use and the impact on the environment. It is well known that climate change is a consequence of CO_2 emissions and other greenhouse gases. In order to turn the situation around, the European Union (EU) has set itself targets for reducing its greenhouse gas (GHG) emissions progressively until 2050. In this context, climate and energy targets were set in:

- 2020 climate and energy package goals: 20 % improvement in the energy efficiency, increase the share of the renewable energy in the generation mix to 20 % and reduce 20 % of the GHG emissions based on 1990 levels [1].
- 2030 climate and energy framework: similarly as the 2020 goals, but it is in line with the Roadmap 2050, for which at least 27 % of the energy efficiency should be improved, 27 % of the share of renewable energy in the energetic matrix and no less than a 40 % reduction of the GHG emissions [2].

To keep up with the previously mentioned targets, the development and deployment of renewable energy has experienced an immense growth in the last decades, as can be seen in Figure 1.1. Focusing on photovoltaic (PV) technology, such growth is also attributed to lower manufacturing costs. Additionally, these PV installations save more than 53 million tons of CO_2 per year [3].

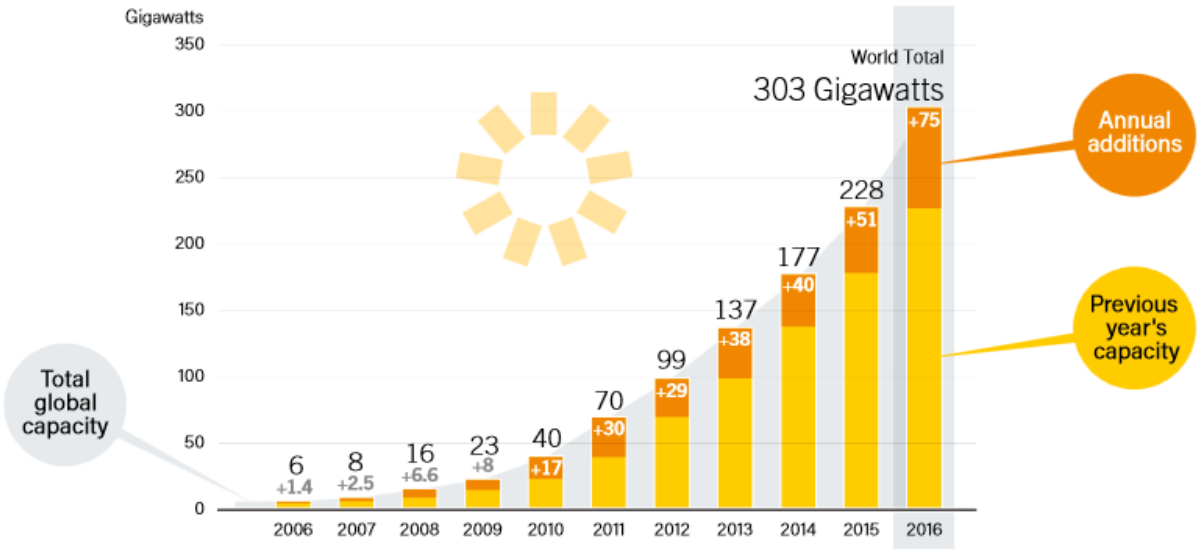

Figure 1.1.: Solar PV global capacity and annual additions 2006-2016 [4].

PV energy will need to play a significant role in the world's energy mix in order to help achieve the 2050 global climate change goals at the lowest cost. According to [5] , by 2050 PV is expected to provide 11 % of the annual global electricity production.

It is known that buildings account for approximately 40 % of energy consumption and 36% of CO_2 emissions in the EU [6]. For this reason, the building sector has big potential in terms of energy savings. A possible solution are the building integrated photovoltaics (BIPV), in which solar panels are used as roofs or walls, hence they not only produce electricity but also reduce the amount of other construction materials needed.

The main goal of this thesis is to develop a domestic PV system with energy storage and a DC/AC inverter. Based on real measured data of irradiance and temperature and by means of the Perez model (used for calculating the incident irradiance on a tilted plane) a simulation model of a PV module is constructed in Simulink. Moreover, a lithium-ion battery is modeled in MATLAB by means of power balances taking into consideration aging effects and finally an inverter is modeled by means of a mathematical model due to speed purposes, given that lots of real measured data is being handled. Furthermore, four operational modes are implemented and a sensitivity analysis is carried out. Special attention has been given to designing the models in a way that they allow easy and flexible configuration, therefore limiting the barrier of entry for possible users.

1.1. Thesis organization

Chapter 2 presents the problem description and the proposed approach is explained. The current state of the art of the modeled components is explained and discussed in **Chapter 3**. **Chapter 4** presents the developed models, while **Chapter 5** provides the reader with a summary of the obtained results and the discussion of them. Finally a conclusion and outlook are provided in **Chapter 7**.

2. Problem description

The need for obtaining and using cleaner ways of energy production has experienced a rapid growth over the last decade. Such increasement has mainly been caused by the need to reduce air pollution, diminish global warming and decrease the dependence on fossil fuels, while at the same time jobs and industries are created and the energy matrix is diversified.

But as renewable energy rapidly grows, with record numbers of wind and solar installations, the main problem and weakness of this technology emerged, namely intermittency and reliability. Renewable energy relies on the weather for its source of power, i.e. if weather conditions are not good enough, renewable energy technologies will not be able to harvest enough energy. In this context, a widely used solution is to store produced energy, so that it is still possible to supply energy to the loads when weather conditions otherwise would not allow to produce enough energy or none at all (e.g. nighttime, cloudy or rainy weather). Energy storage is a key factor in renewable energy plants. It can mitigate power variations, enhance the system flexibility, and enable storage and dispatching of the generated electricity by variable renewable energy sources such as wind and solar [7].

The aim of this thesis is to develop a domestic photovoltaic system, which will be connected to the grid but will not be able to inject the surplus energy back into the grid[1]. The function of the grid in this system will merely be for backup reasons, i.e. in case the battery and PV module are not capable of supplying enough energy to the loads. In the presented system, all components are be modeled using Simulink (the PV module) and MATLAB scripts for the simulation and modeling of the battery and the inverter.

[1]Because the aim of the start-up company is to develop a plug and play battery, i.e. the user just needs to connect it directly to its PV system without having the need to do all the legal work [8] (valid only for Austria and Germany) that involves having a PV system that does inject the surplus power to the grid.

2.1. Embedding the Master Thesis in the P^3P

The present work is part of a bigger project for the development of a product of a start-up company settled in Graz, Austria. Said company is developing a plug and play battery for PV applications, which consists of a mini-solar power plant and a battery, which is characterized by its ease of installation, i.e. the user just needs to plug or connect the battery into the socket (hence the name of the product). The start-up's project consisted in three parts:

1. Functional PV-module, i.e. a PV model that is able to simulate the behavior of a real PV module.
2. General model, which implements the remaining elements of the PV-system (energy storage, the power conditioning unit or the inverter and the loads), perfoms a validation and a sensitivity analysis used for the system's sizing.
3. Control strategies, to improve the functioning of the system.

Note that the scope of the present Master Thesis comprises the development of the functional PV-module and the general model, including the aging effects on the battery. However, literature review has been carried out regarding control strategies that are currently used in PV applications.

2.2. Approach

A simulation model of a general PV module is developed and constructed in Simulink, with inputs being the solar irradiance and ambient temperature. The PV model is able to operate at the maximum power point (MPP), by finding this point the system power output is optimized. Energy storage, more specifically a lithium-ion battery as well as the inverter are modeled and implemented in order to simulate the behavior of the whole system.

More precisely, as previously mentioned due to speed purposes, the output of the PV model was used to generate two curves and their corresponding mathematical functions, a similar procedure is developed with the inverter model, which takes raw data provided by the company and the university, which was needed in the same way for curve fitting. For the battery model, a script based on power balances, offering four types of operational

modes is modeled. At the same time, a degradation model based on the number of cycles, the SOC and the DOD was included.

Lastly, a sensitivity analysis is performed, to determine the influence of varying the standard parameters of the model, such as the inclination, orientation and area of the PV module, the battery's capacity and the inverter's maximum power. This analysis enables to establish a set of parameters yielding in the best possible configuration given the considered scenario. Therefore, the energy having to be purchased from the grid is minimized, which directly translates to saved money for the user.

3. State of the art

This chapter is devoted to performing literature review about each of the elements of the proposed system and to further show the current state of each technology and present the most important definitions.

3.1. Photovoltaic technology

Photovoltaics is the field of technology dealing with devices which convert sunlight (photons) directly into electricity (voltage), therefore its name is given from this process, by means of the so-called "photovoltaic effect".

When talking about PV systems, two main configuration types can be distinguished: stand-alone PV systems and grid-connected PV systems.

Stand-alone PV System

The most common configuration of a stand-alone photovoltaic system (shown in Figure 3.1), consists of [9]:

- PV generator, which includes the whole assembly of solar cells, connections, protective parts, supports, etc.
- Power electronics, such as a DC/AC inverter. It facilitates the integration with the utility grid, given that PV generators produce DC power and most household loads consume AC power. Additionally, the inverter ensures that the solar cells operate at the optimal working point, it monitors the grid and the output of the PV system [10].
- Energy storage, or more specifically a battery. It is a crucial element in the integration of renewable sources, because it does not only reduce power fluctuations

and enhances the flexibility of the electric system but it also enables storage and dispatchability of the generated electricity, making the system more reliable.

- Loads, which are gadgets, devices or appliances that consume electrical power.

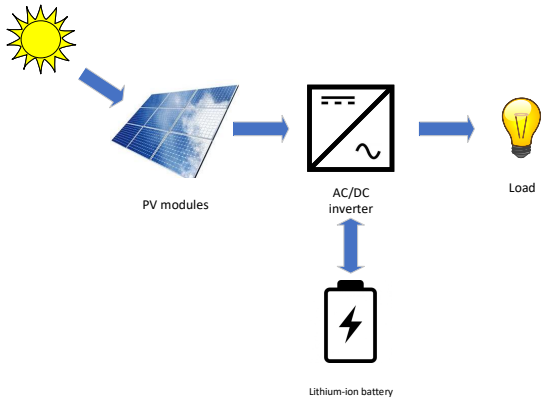

Figure 3.1.: Main layout of a domestic stand-alone PV system.

Grid-connected PV System

Grid-connected PV-systems use the same components as stand-alone systems, with the difference that the energy storage is optional, i.e. a battery can be used as a backup in case of insufficient power supply and frequent interruptions [11]. In Figure 3.2 it can be seen a two-way grid connection point, i.e. energy can be injected to and from the grid, when there is a surplus of energy or when energy is needed to supply the loads, respectively.

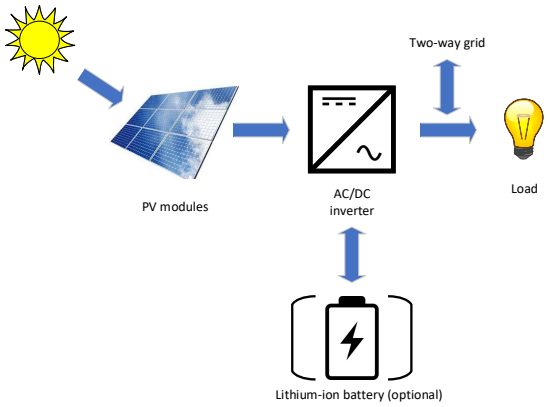

Figure 3.2.: Main layout of a domestic stand-alone PV system.

P^3P PV System

In this work, a new configuration type is used; it results from the combination of a stand-alone system and a grid-connected system.

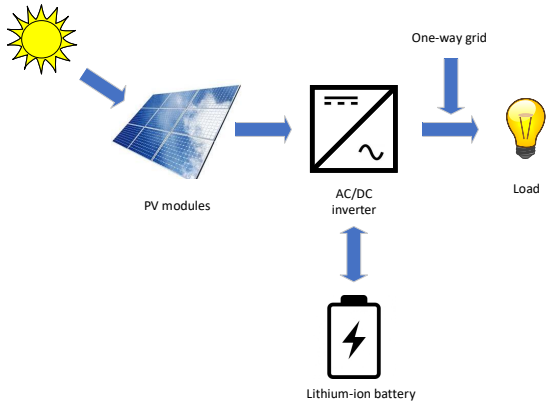

Figure 3.3.: Main layout of a domestic stand-alone PV system.

As depicted in Figure 3.3, the connection with the grid is only one way, meaning that excess of energy cannot be injected to the grid. In this type, the grid's function is merely used when neither the PV system nor the battery are able to supply the load demand.

3.1.1. Solar cells

Solar cells are electronic devices made of semiconductor materials, usually silicon. For example, a silicon wafer (depicted in Figure 3.4), consists of two layers of photovoltaic material, metal grids, anti reflection coating and supporting material. They are specially treated to increase conductivity, such treatment consist of adding impurities (doping), of which there are two types of impurities [12]:

- Acceptor impurities: consist of phosphorous atoms, which have five valence electrons (one more than silicon). The electrons donate weakly bound valence electrons to the silicon material, creating excess negative carriers [13]. Therefore, resulting in the n-type region, which has a much higher concentration of electrons than holes.
- Donor impurities: consist of boron atoms, which have three valence electrons (one less than silicon). In this case the electrons create a greater affinity than the silicon to attract electrons [13], i.e p-type region, which has a higher concentration of holes.

As each type has a different concentration of holes and electrons, this difference in concentration causes a permanent electric field (directed from n-type to p-type). The purpose of this electric field is to separate additional holes (photogenerated positive charge carriers) from electrons (negative counterpart) when the light falls on the cell [14]. Therefore once the circuit is closed on an external load, electrical current is extracted into the load.

Another important element of the solar cell are the metal grids, which enhance the current collection from the front (metal grid with the shape of a comb, so that as much sunlight as possible is harvested by the solar cell) and the back (fully metallized for charge carrier collection) of the solar cells. Finally, anti reflection coating is applied to the top of the cell to maximize the light going into the cell [15].

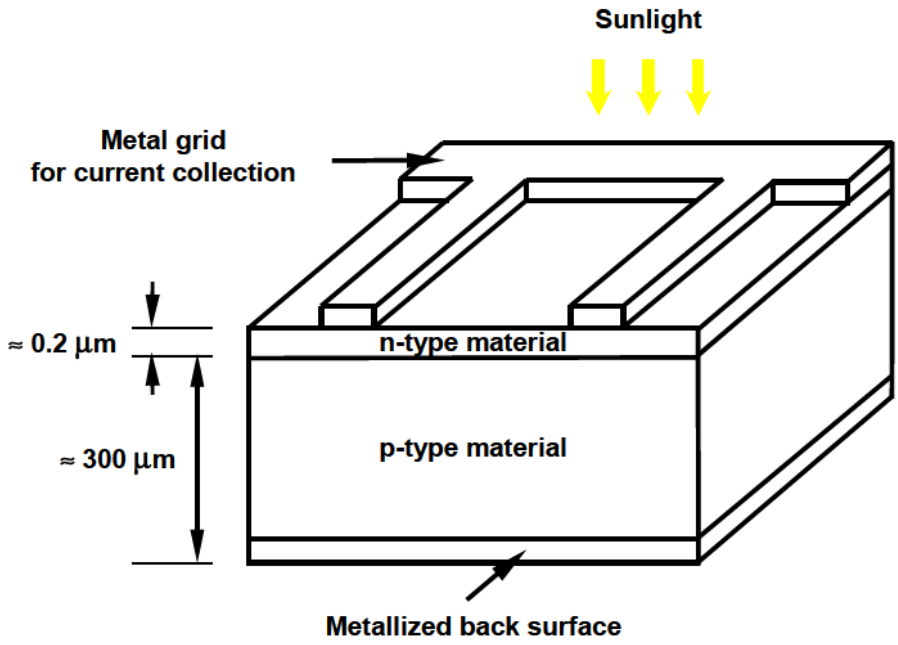

Figure 3.4.: Solar cell structure, approximately 300 µm silicon wafer with a p-n junction made by two layers: p-type material and n-type material [12].

It is worth mentioning that a PV module consists of photovoltaic cells connected together, while a PV array consists of PV modules connected together.

3.1.1.1. Available PV cell technologies

In the following, a brief description of each of the presented PV cell technologies will be provided [16]:

1. **Monocrystalline Silicon modules:** the most expensive (due to the "Czochralski process", a manufacturing process) and the most efficient commercially available module (16-21%), these solar panels yield the highest power outputs, thus requiring the least amount of space (compared to other cells types). They present an energy payback of three years.

2. **Polycrystalline Silicon modules:** also known as polysilicon (p-Si) and multi-crystalline silicon (mc-Si), they perform slightly worse than the monocrystalline modules at higher temperatures and have a lower efficiency range (13-18%), additionally they are cheaper because they are manufactured using a simpler process.

3. **Thin-Film Solar Cells:** also known as thin-film photovoltaic cells or TFPV. Their main characteristic is that they are formed by depositing one or several "thin" layers of a determined PV material onto a substrate. According to the deposited material they can be classified as: Amorphous Silicon (a-Si), Cadmium Telluride (CdTe), Copper Indium Gallium Selenide (CIS/CIGS) or Organic Photovoltaic Cells (OPC). For example, the energy payback of a a-Si cell is about 1 year.

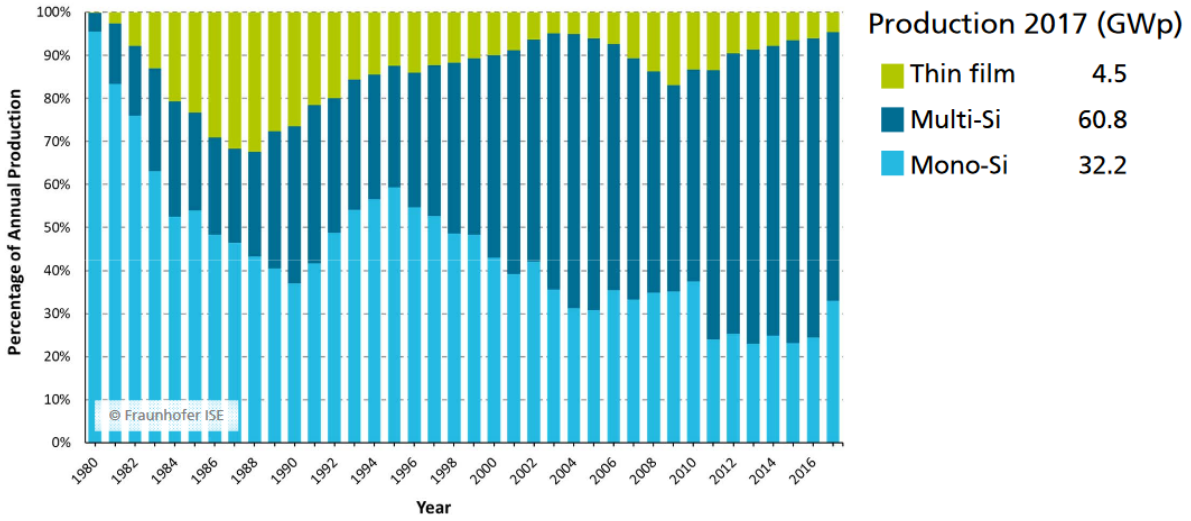

Figure 3.5.: Global PV production by technology and its evolution in the last decades [17].

Figure 3.5, depicts the global PV production and its evolution between the 80s and 2017, it can be seen that the polycrystalline technology is preferred over the monocrystalline modules, mainly because mc-Si modules are a cost effective solution with reasonable efficiency ranges.

3.1.2. PV module modeling

The following subsection is devoted to present the different ways of which a PV module can be modeled, starting from the most simplest model to a model that resembles the behavior of a real module.

3.1.2.1. Ideal single model

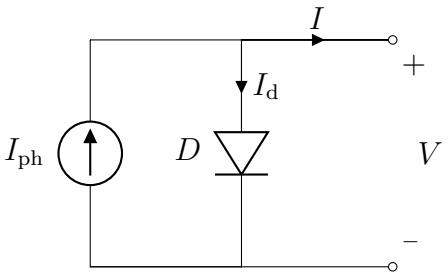

Figure 3.6.: Ideal single diode model (Own elaboration based on [18]).

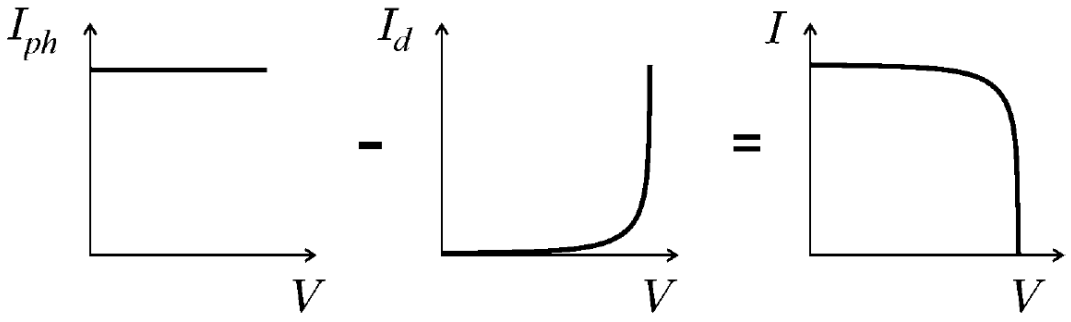

Figure 3.7.: I-V characteristic curve of an ideal PV cell when applying the Kirchoff's law to the circuit in Figure 3.6 [19].

Figure 3.6 shows the equivalent circuit of the simplest way to model a PV module, it consists of a diode connected in parallel with the light generated current source, the latter one describes the conversion of luminous flow into electric energy while the diode describes the behavior of the cell's junction [18,20]. Following Kirchoff's law, the output current of a PV module (as depicted in Figure 3.7), can be modeled as

$$I = I_{\mathrm{ph}} - I_{\mathrm{d}}\,, \tag{3.1}$$

$$I_{\mathrm{d}} = I_{\mathrm{o}} \cdot \left[\exp\left(\frac{V}{a}\right) - 1\right]\,, \tag{3.2}$$

$$V_{\mathrm{T}} = \frac{k \cdot T_{\mathrm{c}}}{q}\,, \tag{3.3}$$

$$a = \frac{N_{\mathrm{s}} \cdot A \cdot k \cdot T_{\mathrm{c}}}{q} = N_{\mathrm{s}} \cdot A \cdot V_{\mathrm{T}}\,, \tag{3.4}$$

where I is the output current, I_{ph} the photogenerated current, I_{d} is the diode current, V the output voltage, T_{c} the cell temperature, N_{s} the number of PV cells connected in series, A represents the ideality factor, which depends on the PV technology, as can be seen in Table 3.1, a is the modified ideality factor, k the Boltzmann constant[1] and q is the electron constant.[2]

Table 3.1.: Ideality factor for different PV technologies [21].

PV technology	Ideality factor "A"
Si-mono	1.2
Si-poly	1.3
a-Si-H	1.8
a-Si-H tandem	3.3
a-Si-H triple	5
CdTe	1.5
CIS (Copper, Indium and Selenium)	1.5
AsGa	1.3

[1] k=1.381 $\times 10^{-23}$ [J/K]
[2] q=1.602 $\times 10^{-19}$ [C]

3.1.2.2. Practical model with R_s

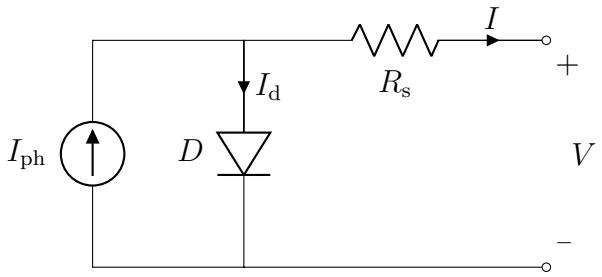

Figure 3.8.: Practical single diode model with a series resistance (Own elaboration based on [18]).

A new element is introduced in this way of modeling a PV module: a series resistance, as can be observed in Figure 3.8, which shows the equivalent circuit of this model. It presents better accuracy than the ideal model, but still presents some deficiencies when varying the temperature. In this case the fill factor is reduced, because a slight voltage drop is caused by the series resistance, its value is usually very small [20].

3.1.2.3. Practical model with R_s and R_p

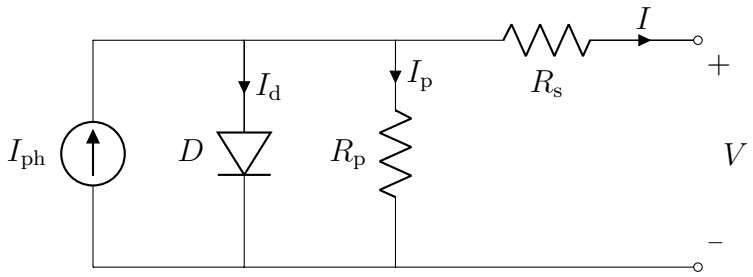

Figure 3.9.: Practical single diode model with series and parallel resistances (Own elaboration based on [18]).

For this case, not only a series resistance is included but also a parallel or shunt resistance. The equivalent circuit of this model can be observed in Figure 3.9. Unlike R_s, R_p generally has a quite high resistance (For example [19] considers $R_p = 415.4\Omega$, while the $R_s = 0.22\Omega$). Its highest effect occurs when light levels are low, because when there is a small photogenerated current, the current flowing through R_p will be higher compared to the total and the voltage does not change much with irradiance. This is the improved model of

the two previously discussed models, because it introduces two elements that approximate the model closest to a real device. The series resistance appears from the bulk resistance of the silicon wafer, metallic contacts of the front and back surface and other parasitic elements from connections and terminals. On the other hand, the parallel resistance is mainly caused by leakage currents due to the p-n junction, non-idealities and impurities near the junction, especially near the cell edges [12,19,20]. It can be modeled as [18,19]

$$I = I_{\mathrm{ph}} - I_0 \cdot \left[\exp\left(\frac{V + I \cdot R_{\mathrm{s}}}{a}\right) - 1\right] - \frac{V + R_{\mathrm{s}} \cdot I}{R_{\mathrm{p}}}\,, \tag{3.5}$$

$$I_{\mathrm{ph}} = \frac{G}{G_{\mathrm{n}}}\left(I_{\mathrm{ph,n}} + k_{\mathrm{i}} \cdot \Delta T\right)\,, \tag{3.6}$$

$$I_{\mathrm{ph,n}} = \frac{R_{\mathrm{p}} + R_{\mathrm{s}}}{R_{\mathrm{p}}} \cdot I_{\mathrm{sc}}\,, \tag{3.7}$$

where R_{s} and R_{p} are the equivalent series and parallel resistances in [Ω] of the photovoltaic module, G is the irradiance on the photovoltaic's surface in [$\mathrm{W/m^2}$] and G_{n} represents the nominal irradiance ($1000\,\mathrm{W/m^2}$).

3.1.3. Solar radiation

The total or global radiation consists of three components: beam, diffuse and ground reflected radiation.

When the solar radiation goes through the atmosphere, part of the incident energy is either absorbed by air molecules or scattered. The radiation which is not reflected or scattered (i.e. the remaining radiation) and that reaches the surface is called direct or beam radiation. The scattered radiation that reaches the ground is known as diffuse radiation. Lastly, the radiation that arrives at the panel after reflection from the ground is called ground reflected radiation [22], this concept is depicted in Figure 3.10.

3.1.4. Radiation model: The Perez algorithm

The Perez model is the one of the most widely used models. It tries to replicate the sky conditions by dividing diffuse radiation from the sky dome into three components. The

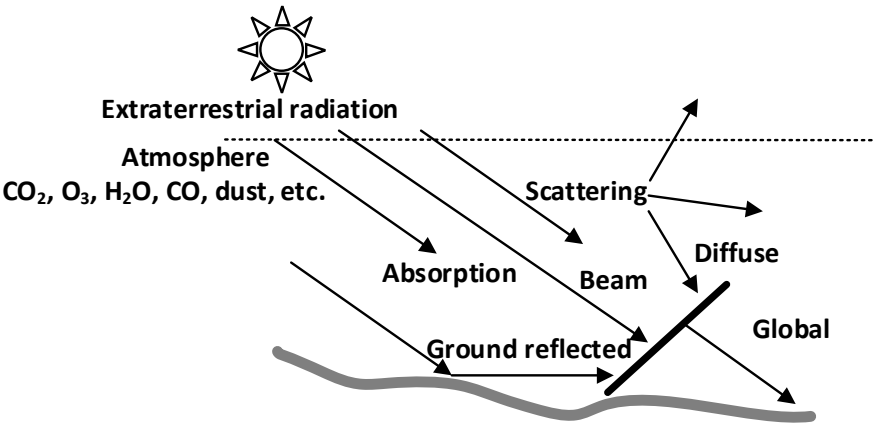

Figure 3.10.: Solar radiation components [23].

advantage of using the Perez model is that it analyzes the diffuse components in more detail (c.f. Figure 3.11) [24,25]:

- **Isotropic component**, which represents the uniform irradiance from the sky dome.
- **Circumsolar diffuse component**, which represents the forward scattering of radiation concentrated in the area immediately surrounding the sun, i.e. centered at the position of the sun.
- **Horizon brightening component**, which is assumed to be a linear source at the horizon and to be independent of the azimuth.

The effect of these three components can be easily seen in (3.8), this equation shows the diffuse on a tilted surfaced, the first term is the isotropic diffuse, the second is the circumsolar diffuse and the third is the diffuse from horizon [22],

$$I_{\mathrm{d,T}} = I_{\mathrm{d}} \cdot \left[(1 - F_1) \cdot \left(\frac{1 + \cos\beta}{2} \right) + F_1 \cdot \frac{a}{b} + F_2 \cdot \sin\beta \right] , \tag{3.8}$$

where $I_{\mathrm{d,T}}$ is the diffuse radiation on a tilted collector, the remaining parameters are going to be explained in detailed in the following.

In order to solve the previous equation and having the pertinent descriptions of the Perez Model (based on [22]), the following algorithm is proposed:

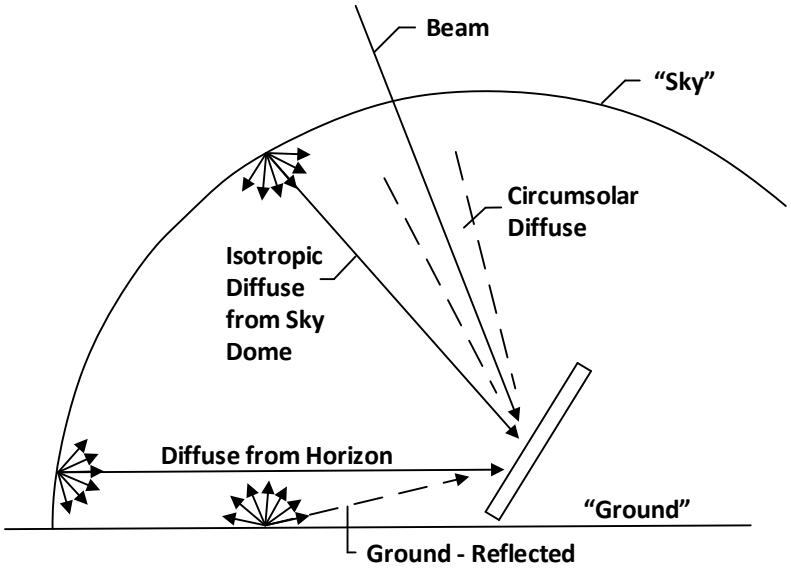

Figure 3.11.: Diffuse components on a tilted surface [22].

1. **Input parameters:**
   - I = measured solar irradiance on a horizontal surface [W/m^2]
   - n = day of the year
   - x = hour of the day
   - G_{sc} = solar constant = 4.92 [MJ/m^{2}h]
   - β = inclination of the surface [°]
   - ϕ = latitude [°]
   - γ = surface azimuth angle (surface's orientation) [°]
   - ρ_{g} = ground reflection (e.g 0.6 or 0.7 for fresh snow)
2. **Declination's calculation:** the declination [°] is the angular sun's position when the sun is on the local meridian with respect to the equator's plane, it is given by

$$\rho = 23.45 \sin\left(360 \cdot \frac{284 + n}{365}\right), \tag{3.9}$$

where $n \in [1, 365]$ and the declination oscillates between $-23.45° \leq \delta \leq 23.45°$.

3. **Hour angle calculation:** the hour angle $\omega[^\circ]$ is the angular displacement of the sun east or west of the local meridian due to rotation of the earth on its axis at 15 degrees per hour, calculated using:

$$\omega = (x - 12) \cdot 15\,. \tag{3.10}$$

4. Find the **extraterrestrial radiation** on a horizontal surface I_o for an hour, it can be calculated using

$$\begin{aligned} I_\mathrm{o} = \frac{12 \cdot 3600}{\pi} \cdot G_\mathrm{sc} \left(1 + 0.033 \cos \frac{360 \cdot n}{365}\right) \cdot \\ \left[\cos\phi \cdot \cos\delta \cdot (\sin\omega_2 - \sin\omega_1) + \frac{\pi \cdot (\omega_2 - \omega_1)}{180} \cdot \sin\phi \cdot \sin\delta\right]\,, \end{aligned} \tag{3.11}$$

where G_sc, represents the energy from the sun received on a unit area per unit time; it is perpendicular to the radiation's propagation direction, outside the atmosphere (at a mean earth-sun distance). ϕ is the latitude, defined as the angular location, north or south of the equator, within a range of $-90^\circ \leq \phi \leq 90^\circ$. Note that a positive angle indicates the north. Regarding the hour angle, note that period ω_2 is larger than ω_1.

5. **Clearness index** calculation, which is defined as

$$k_\mathrm{T} = \frac{I}{I_\mathrm{o}}\,, \tag{3.12}$$

in other words, it is the ratio of a the radiation of a particular day to the extraterrestrial radiation for the same day.

6. **Diffuse radiation calculation**, the diffuse radiation I_d is the solar radiation received from the sun but that has been scattered by the atmosphere. It can be calculated by means of Figure 3.12 or by applying Equation (3.13),

$$\frac{I_\mathrm{d}}{I} = \begin{cases} 1.0 - 0.09\,k_\mathrm{T} & \text{for } k_\mathrm{T} \leq 0.22 \\ 0.9511 - 0.1604\,k_\mathrm{T} + 4.388\,k_\mathrm{T}^2 & \\ \quad - 16.638\,k_\mathrm{T}^3 + 12.336\,k_\mathrm{T}^4 & \text{for } 0.22 < k_\mathrm{T} \leq 0.80 \\ 0.165 & \text{for } k_\mathrm{T} > 0.80 \end{cases} \tag{3.13}$$

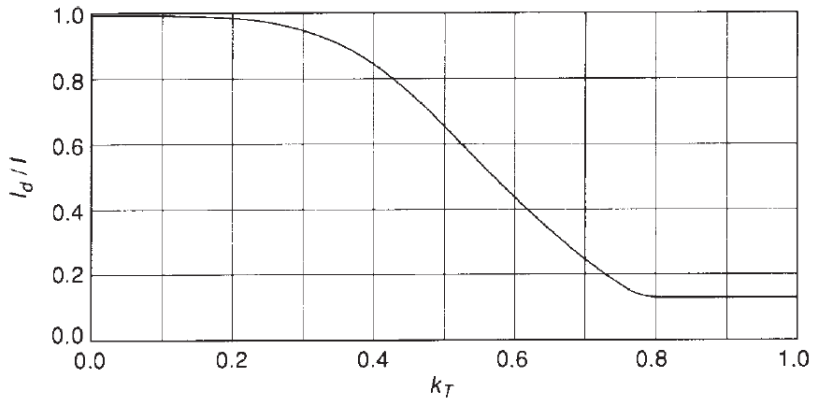

Figure 3.12.: I_d/I ratio as a function of the clearness index [22].

7. **Direct beam calculation:**

$$d = \frac{I_\mathrm{d}}{I}\,, \tag{3.14}$$

$$I_\mathrm{b} = I \cdot (1 - d)\,, \tag{3.15}$$

where d is the ratio between the diffuse radiation and the radiation of a particular day. I_b represents the beam radiation, it is the "total solar radiation"[3] that is received from the sun. This means it has not been scattered by the atmosphere, it is also known as direct solar radiation.

8. Find the **zenith angle** and **angle of incidence:**

$$\cos\theta_z = \cos\phi\cos\delta\cos\omega + \sin\phi\sin\delta\,, \tag{3.16}$$

$$\begin{aligned}\cos\theta = {} & \sin\delta\sin\phi\cos\beta - \sin\delta\cos\phi\sin\beta\cos\gamma \\ & + \cos\delta\cos\phi\cos\beta\cos\omega + \cos\delta\sin\phi\sin\beta\cos\gamma\cos\omega \\ & + \cos\delta\sin\beta\sin\gamma\sin\omega\,,\end{aligned} \tag{3.17}$$

where θ represents the angle of incidence and is defined as the angle between the beam radiation on a surface and the normal to said surface while θ_z is the zenith angle and represents the angle of incidence on a horizontal surface of the beam radiation. γ is the surface azimuth angle, which is the angle made in the horizontal

[3]The total solar radiation is defined as the sum of the beam and diffuse solar radiation on a surface.

plane of the normal to the surface from the local meridian, it is bounded by $-180° \leq \gamma \leq 180°$. Negative angles represent east orientation while positive ones represent west orientation and for $\gamma = 0$ it would be a south orientation, finally, β is the angle between the surface's plane and the horizontal plane, therefore $0° \leq \beta \leq 180°$. The representation of these angles can be easily observed in Figure 3.13.

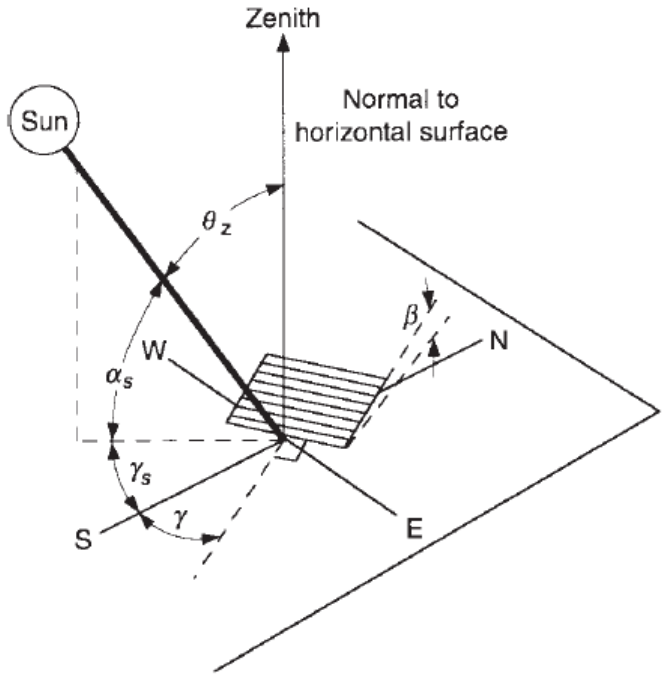

Figure 3.13.: Representation for a tilted surface of the Zenith angle, slope surface's azimuth angle and solar azimuth angle [22].

9. The **geometric factor** can be calculated using

$$a = \max(0, \cos\theta)\,, \tag{3.18}$$

$$b = \max(\cos 85°, \cos\theta_z)\,, \tag{3.19}$$

$$R_\mathrm{b} = \frac{a}{b}\,, \tag{3.20}$$

where a and b represent the angles of incidence of the cone of circumsolar radiation (c.f. Figure 3.11) and R_b represents the ratio between the beam radiation on a tilted plane and the radiation of the plane of measurement, which is usually horizontal.

10. Calculation of the **extraterrestrial normal incidence radiation**, I_on represents the extraterrestrial radiation incident on the plane normal to the radiation on a

specific day of the year,

$$I_{\text{on}} = G_{\text{on}} = \begin{cases} G_{\text{sc}} \left(1 + 0.033 \cdot \cos \frac{360 \cdot n}{365}\right) \\ G_{\text{sc}}(1.000110 + 0.034221 \cos B + 0.001280 \sin B \\ \qquad + 0.000719 \cos 2\,B + 0.000077 \sin 2\,B) \end{cases} \tag{3.21}$$

Note that in the lower equation in (3.21) a new term appears: B (calculated using (3.22)) This is a more accurate equation ($\pm$ 0.01%), but it should also be noted that the upper equation has an adequate accuracy for most engineering calculations [22].

$$B = (\text{n} - 1) \cdot \frac{360}{365} \tag{3.22}$$

11. Finding the the **air mass**, by

$$m = \frac{1}{\cos \theta_{\text{z}}}\,, \tag{3.23}$$

where m is the air mass, defined as the length of the path transversed by the beam radiation in reaching the sea level when the sun is at its zenith.

12. **Brightness parameter** or also commonly seen in literature as sky brightness, is given by

$$\Delta = m\,\frac{I_{\text{d}}}{I_{\text{on}}}\,, \tag{3.24}$$

where Δ represents the sky brightness.

13. **Normal incidence beam radiation**, defined as the ratio between the beam radiation and the zenith angle,

$$I_{\text{b,n}} = \frac{I_{\text{b}}}{\cos \theta_{\text{z}}}\,. \tag{3.25}$$

14. Calculation of the **sky clearness** or clearness parameter, calculated as

$$\epsilon = \frac{\frac{I_d + I_{b,n}}{I_d} + 5.535 \times 10^{-6} \cdot \theta_z^3}{1 + 5.535 \times 10^{-6} \cdot \theta_z^3}\,, \tag{3.26}$$

where ϵ is a function of the diffuse radiation at a given hour and $I_{\mathrm{b,n}}$.

15. Find the **brightness coefficients** F1 and F2, more specifically the circumsolar and horizon brightness coefficients, using Table 3.2 and

$$F_1 = \max\left\{0, \left(f_{11} + f_{12} \cdot \Delta + \frac{\pi}{180^\circ} \cdot \theta_z \cdot f_{13}\right)\right\}\,, \tag{3.27}$$

$$F_2 = f_{21} + f_{22} \cdot \Delta + \frac{\pi}{180^\circ} \cdot \theta_z \cdot f_{23}\,. \tag{3.28}$$

Table 3.2.: Brightness coefficients for Perez Anisotropic Sky [22].

Range of ϵ	f_{11}	f_{12}	f_{13}	f_{21}	f_{22}	f_{23}
1.000 to 1.065	-0.008	0.588	-0.062	-0.060	0.072	-0.022
1.065 to 1.230	0.130	0.683	-0.151	-0.019	0.066	-0.029
1.230 to 1.500	0.330	0.487	-0.221	0.055	-0.064	-0.026
1.500 to 1.950	0.568	0.187	-0.295	0.109	-0.152	0.014
1.950 to 2.800	0.873	-0.392	-0.362	0.226	-0.462	0.001
2.800 to 4.500	1.132	-1.237	-0.412	0.288	-0.823	0.056
4.500 to 6.200	1.060	-1.600	-0.359	0.264	-1.127	0.131
6.200 to ∞	0.678	-0.327	-0.250	0.156	-1.377	0.251

16. Compute the **diffuse sky irradiance** on the tilted plane, using (3.8), furthermore it is possible to calculate the **total radiation** I_{T} (which includes two extra terms: the beam and the ground reflected components) on the tilted surface,

$$\begin{aligned} I_{\mathrm{T}} = I_{\mathrm{b}} \cdot R_{\mathrm{b}} + I_{\mathrm{d}} \cdot (1 - F_1) \cdot \left(\frac{1 + \cos\beta}{2}\right) + I_{\mathrm{d}} \cdot F_1 \cdot \frac{a}{b} \\ + I_{\mathrm{d}} \cdot F_2 \cdot \sin\beta + I \cdot \rho_{\mathrm{g}} \cdot \left(\frac{1 - \cos\beta}{2}\right)\,. \end{aligned} \tag{3.29}$$

3.2. Energy storage in photovoltaic systems

PV electricity is generated in a non constant way, varying from a maximum peak during sunshine hours to no production during night time. Some energy applications are suited

for these sunshine periods (and so energy is directly taken from the PV modules), while others require a continuous amount of energy supply, regardless the time of the day; for the latter applications, a reliable energy storage system (EES) needs to be implemented.

While the primary function of a storage system is to provide power when sunlight is not available, thus increasing the fraction of time the PV system provides electricity, the inclusion of batteries has many other advantages, meaning that batteries can be used for multiple purposes. For example, for small systems consisting of one or two PV modules, batteries can function as a load-matching system. Another case is, in PV systems which contain a load with a large initial current draw (such as experienced by an inductive load, typically a motor), the batteries can be utilized to provide the initial start-up current. In grid-connected systems, it can be used for peak shifting, in this case the power generated by the sun is stored for several hours in order to better match when the peak load occurs [26].

Among the types of energy storage systems, there are [27]:

- Electrochemical storages (hydrogen and flow batteries) and secondary batteries.
- Mechanical storages like flywheels.
- Electromagnetic storages, such as supercapacitors and superconducting magnetic energy storage (SMES). These storage types are the less relevant for PV applications, given that supercapacitors and SMES are considered high-power systems and short term storages (i.e. in the range of seconds and minutes), therefore are used for stability reasons.

Secondary batteries are the most suitable and commonly used type of energy storage (ES) for PV applications, the following section will be devoted to these type of ES [28].

The batteries used in PV applications have a different working approach, when compared to stationary or motive power applications. They are characterized by a small or fractional change in the state of charge (SOC) on a daily basis, meaning that they go through several charge/discharge cycles and present some sharp decline in SOC in some periods of the year, in other words they depend on the weather and season [29].

Additionally, typical stand alone PV systems require strength, resistance, environmental flexibility, easy installation, reliability and the capability of unattended operation. Thus, the selected battery should also fulfill the same requirements and match the following characteristics [30]:

- High cycle life
- High capacity at slow discharge rate
- Good reliability under cyclic discharge conditions
- High energy efficiency at different SOC levels
- Low self-discharge
- Wide operating temperature range
- Long life, robust design and low maintenance requirements
- Highly cost effective
- Manufactured under rigorous quality controls

3.2.1. Important battery characteristics

In the following, some of the most important battery's characteristics are discussed, to ease understanding of the following sections and chapters [31,32].

- State of Charge (SOC) is the remaining capacity of the battery to store energy with respect to its full load state. It depends on the nominal battery's capacity in [Ah], current, temperature, charge and discharge. Mathematically, is defined as the ratio between the available battery charge at a given time divided by the maximum capacity,

$$\mathrm{SOC} = \frac{Q}{C}\,. \tag{3.30}$$

- Current Depth of Discharge (DOD), is the reverse of the state of charge,

$$\mathrm{DOD} = \left(1 - \frac{Q}{C}\right)\,. \tag{3.31}$$

  Additionally, it should be mentioned that there is a relationship between maximum DOD and the cycles, i.e. the smaller DOD the larger number of cycles (as depicted in Figure 3.14). As can be observed in Figure 3.15, the maximum usable battery's capacity (or SOC) for a given maximum DOD. For example,a DOD of 90%, means that the battery's SOC is limited to 90% and having 10% unused.

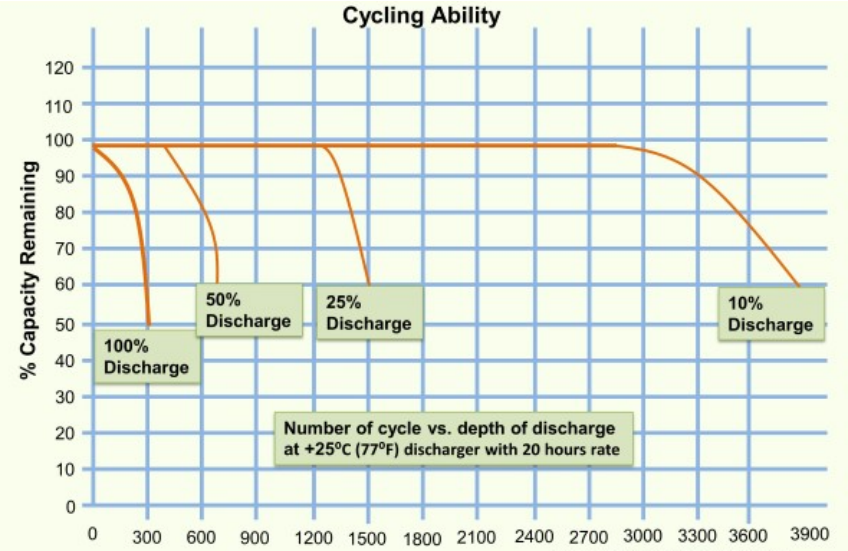

Figure 3.14.: Influence of the DOD over the number of cycles of a battery [33].

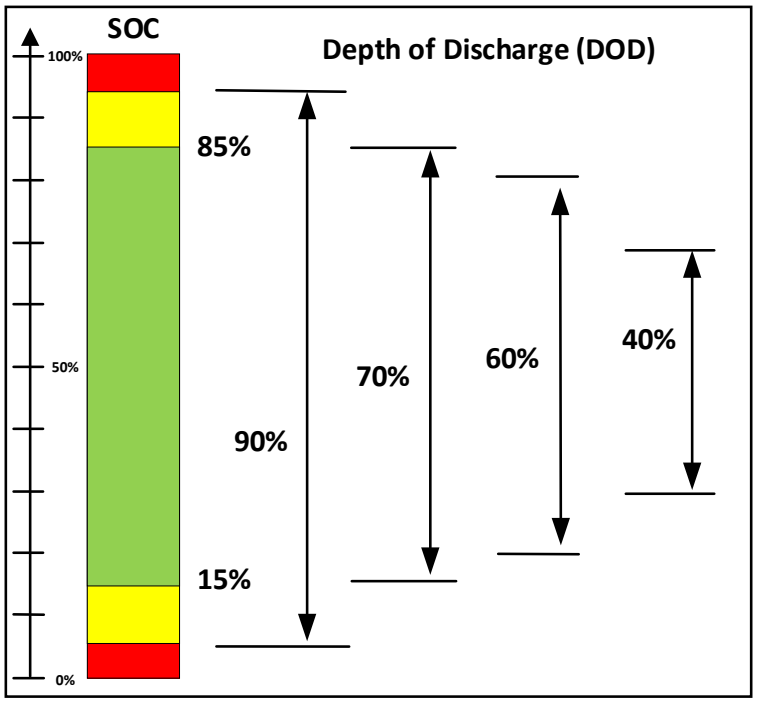

Figure 3.15.: Influence of the DOD over the SOC of a battery [34].

- State of Health (SOH) is a measure of the available battery capacity with respect to its nominal or rated capacity (which is shown in the name plate) while brand new.

- Energy capacity, is defined as the usable energy at a defined discharge rate, the latter term is commonly indicated in [Ah].
- Specific energy density, defined as the amount of possible energy (Wh) storable per kilogram. In other words it relates the energy capacity with the battery weight.
- Specific power density, it represents the amount of power storable per kilogram (W/kg).
- Battery nominal capacity is defined as the total charge that can be stored. Given by the manufacturers for certain measurement conditions, usually consisting of measuring the charge delivered by the battery in a given period of time at a given discharge rate and temperature.
- Self-discharge is the rate at which the battery discharges when not used, mainly due to parasitic conductance within the cell, side-reactions, impurities, among others.

3.2.2. Secondary batteries

Batteries are devices that deliver and take electrical energy and store it in form of chemical energy; secondary batteries are characterized for being cycled, meaning that they can be charged and discharged a number of times until the end of its useful lifetime. In secondary batteries, the conversion of electrical to chemical energy and vice versa happens when electrons are donated (oxidation) or accepted (reduction). These reactions are the so-called redox reactions and occur both at the positive and negative electrodes, known as cathode and anode, respectively. The difference between these two electrodes results in the cell's voltage. Furthermore, the anode and the cathode work both as the energy conversion and the energy storage site; both of them must be good electron and ion conductors. Apart from the two electrodes, another component is the electrolyte, whose objective is to support the transfer of ions between the electrodes and at the same time prevent the electrons to flow between electrodes, which instead follow an external path of the cell via current collectors, enabling them to work (see Figure 3.16). Lastly, a separator (made of a porous and electronically isolating material) between the two electrodes avoids the direct contact between the electrochemical active substances in the anolyte and the catholyte regions, thus preventing the battery from an internal short-circuit [31,35].

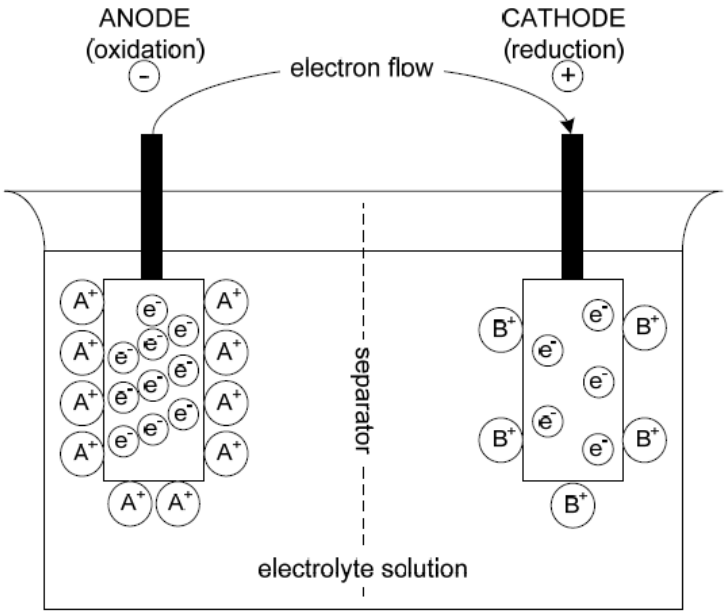

Figure 3.16.: Redox reactions in secondary batteries and depiction of the battery's components [31].

3.2.2.1. Lead-Acid batteries

The Lead-Acid (LA) battery was the first type of secondary battery to be developed, invented by a french physicist (Gaston Plantè) in 1859. Over the decades it has been used for numerous applications such as starting batteries, backup power batteries, telecommunication batteries, traction batteries and nowadays as storage of energy produced by renewable sources. The principal advantages and disadvantages of the LA batteries [36] are presented in the following summary.

Advantages:

+ Low cost
+ Recyclable
+ Available in maintenance-free options
+ Easy to manufacture in high-volume production
+ Good recharge efficiency (over 70 %)
+ Available in a variety of capacities, sizes and designs

+ Good high-rate performance
+ Wide operating temperature range (−40 °C to 60 °C)
+ Good single cell voltage (open circuit voltage > 2 V)
+ Easy state of discharge/charge indication

Disadvantages:

- Relatively low cycle life (500 deep cycles)
- Long term storage in a discharged condition can lead to battery's electrode sulfation and cause irreversible damage
- Low energy density (typically 30-40 Wh/kg)

3.2.2.2. Nickel-Metal hybride (Ni-MH) batteries

Since 1990, when the first Ni-MH battery was commercialized in Japan, it has been adapted to a wide range of applications from hand-held electronics to electric vehicles (EVs) and hybrid electric vehicles (HEVs). Ni-MH batteries, the so-called green batteries because they are produced without lead (Pb) or cadmium (Cd) pollution, where developed and commercialized aiming some attributes such as high energy density, environmental compatibility, low cost, long life, small size, lightweight and safety, among others [37]. In the following, a summary of the main advantages and disadvantages of the Ni-MH [27,38] is discussed.

Advantages:

+ Better mechanical strength
+ Easy maintenance
+ Long life
+ Low volume and weight
+ Reliability
+ Maturity
+ Good high-rate performance
+ Moderately good operating temperature range (−20 °C to 60 °C)

+ Lesser environmental issues (lesser hydrogen discharge and no spill over issues)
+ High charge and discharge rates

Disadvantages:

- Cost
- Cyclability (800 cycles, 80% DoD, C/8)
- Self-discharge (Monthly self-discharge of 10%)
- Lower cell voltage (1.2 V)
- Higher current consumption for charging
- Higher distilled water consumption than LA batteries

3.2.2.3. Sodium-Sulphur batteries

Sodium Sulfur (NaS) batteries were originally developed by the Ford Motor Company in the 60s and subsequently the technology was sold to the Japanese company NGK. NGK now manufactures battery systems for stationary applications. The advantages and disadvantages of this type of technology [3] are briefly presented.

Advantages:

+ High operation temperature 300 °C to 350 °C (this characteristic can be an advantage for CHP plants)
+ Longer lifetime
+ High energy density (up to three times the energy density of a LA battery)
+ Low maintenance
+ Modularity and scalability
+ No self-discharge
+ Good high-rate performance
+ High energy efficiency (around 90 %)
+ High voltage (open circuit voltage $>$ 2 V)
+ High cyclability (4500 cycles, 80% DoD, 1C)

Disadvantages:

- Long time to turn on
- Cost
- High production and maintenance requirements
- Few manufacturers
- High operation temperatures, for some applications this can be a disadvantage, because reaching this high temperatures can require some time.

3.2.2.4. Lithium-ion batteries

Lithium-ion batteries (LIB) are without doubt one of the enabling technologies for a global energy transition, in which the aim is to decarbonize diferent sectors, such as transport and power systems. Li-ion batteries offer excellent technical benefits for the storage of electricity produced with intermittent renewable energies, either from large generation plants, or from distributed generation on a small scale. Lithium-ion and other lithium-based batteries have the highest energy densities (per unit volume or per unit mass) of all rechargeable batteries. A small summary regarding the drawbacks and advantages of the LIB technology [31] shown in the following.

Advantages:

+ Energy efficient (around 92%)
+ Flexibility
+ Low self-discharge
+ High energy density
+ Cyclability (3000 cycles at 80% DoD, 1C)
+ High cell voltage (3.6 V)
+ High current rates

Disadvantages:

- Cost

- Safety and protection needs, because LIB are sensitive to temperature and its chemistry is complex, thus a protection circuit that is able to protect against overheat, overcharge and overdischarge is required.

After having reviewed the main types of secondary batteries and in order to have a better idea of why LIB are the preferred ones nowadays, Figure 3.17 can be used to show that LIB can store more energy while obtaining a smaller and lighter form factor.

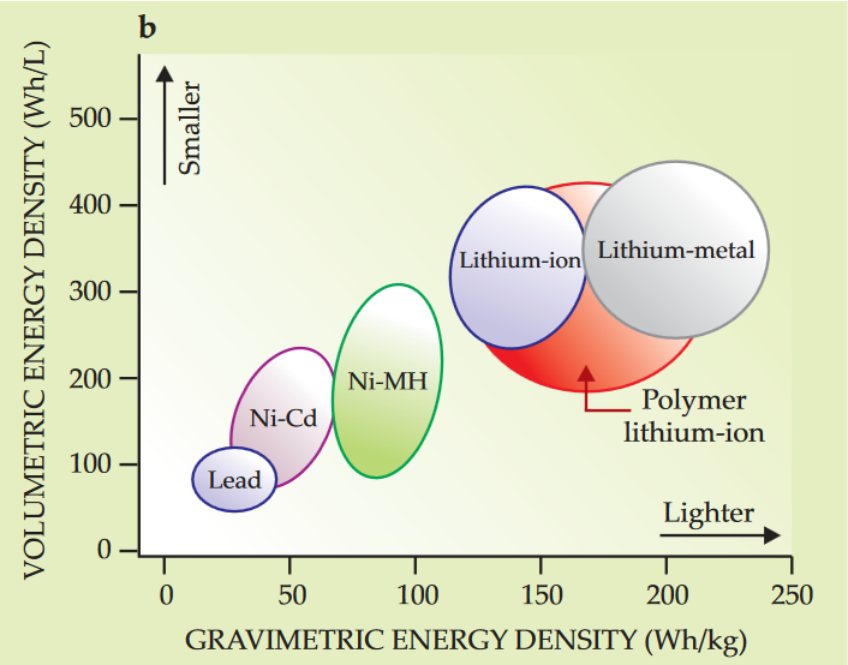

Figure 3.17.: Range of energy density of rechargeable batteries [39].

3.3. Inverters in photovoltaic applications

It is known that PV generators as well as batteries deliver direct current and voltage (DC). Although many small consumers are able to directly operate with DC voltage, that is not the case with most commercial devices which need alternating current (AC). For this reason that power-conditioning devices, like inverters, are needed in PV systems. As their name says, they invert the polarity of the source in the rhythm of the AC frequency. Furthermore, in grid-connected systems inverters are necessary for the conversion of the DC power to a grid-compatible AC power [40].

Power electronics are the technology, whose job it is to process and control the flow of electric energy by supplying optimally suited voltages for user loads. Different types of

inverters produce a different quality of electricity. Therefore, the user must match the power quality required by the loads with the power quality produced by the inverter. Major discrepancies exist between the power produced by PV modules and the grid's requirements [41,42].

Although PV electricity production has experienced a dramatic price reduction over the last years, the role of the conversion efficiency keeps playing a crucial role in the economic and technological point of view of the PV system [43]. Therefore, high efficiency is required by PV inverters (both in grid-connected and stand alone systems), not only when working at nominal power but also during partial load [40].

The efficiency of an inverter indicates how much of the available solar power (in percent) is actually converted and fed into the loads or the utility grid. Advanced inverters currently consume between 4-8 % of the converted energy in the conversion process, which corresponds to an overall efficiency of 92 % to 94 %. Reducing this already low energy consumption represents a big technical challenge, one that can only be overcome with innovative and new inverter designs. [42].

Additionally, PV inverters must also deal with issues related to the PV panels' technology and electrical requirements, such as having galvanic isolations to overcome leakage current related problems in the PV panels interconnections [44]. Also, a maximum power point tracker (MPPT) for irradiance and temperature is required due to the non-linear voltage and current characteristics of the PV-inverter [45]. Lastly, the power quality and the operational characteristics of the PV inverters must comply with the electrical standards of the country where it is installed.

3.3.1. Inverter typologies

There are four different solar PV inverter typologies, that is the different ways of interconnection between PV panels and the inverters [46]:

1. Central inverters, which usually work in the range of several kW to 100 MW.
2. String inverters, typically rated around a few hundred W to a few kW.
3. Multi-string inverters, typically rated around the 1 kW to 10 kW range.
4. Module inverters or micro-inverters, typically rated around 50 W to 500 W.

The following sections are dedicated to describe them, each of these types can be observed in Figure 3.18.

3.3.1.1. Centralized inverters

The most common form of interconnection used in PV systems, is an inverter which is connected to many PV modules. Its conversion efficiency is around 95 % (or even higher) and their unit cost per watt is relatively low. However their main drawbacks are the low levels of reliability and flexibility [42].

3.3.1.2. String inverters

As its name suggests solar modules are connected in series to form a string, the resulting high voltage, high current DC output is then fed into a string inverter. Their peak efficiency oscillates between 96 % and 98 % This is the favorite structure in a new installation and also the most successful technology, because it uses Metal Oxide Field Effect Transistors (MOSFET) or Insulated Gate Bipolar Transistor (IGTB) for performing self-commutated switching actions instead of using thyristors. However, in a partial shading scenario, the maximum power point (MPP) tracking may still not be sufficient to achieve a certain efficiency requirement. Also relatively high cable losses take place due to the flow of high current that interconnects the modules and feeds the output to the string inverter [42,47].

3.3.1.3. Multi-string inverters

In this type of inverter, DC-DC converters are implemented in each string, with the purpose of power combining different strings to a DC bus and MPP tracking. Their advantage is that they present an optimal MPPT for single string of PVs. Furthermore, they are useful when combining PV strings with different orientations and rated power. Such inverters come with very high peak efficiencies, around 99 % [42,47].

3.3.1.4. Module integrated inverters

Also known as micro-inverters, they are a device that integrates into one device, both the PV panel and the micro-inverter are joint together, resulting in a module that generates

grid-compatible AC power. Micro-inverters have a simplified design: a environmentally isolated and enhanced unit. The range of efficiency goes between 94 % and 96 %, in this type the cable losses are lower because power is transported as AC instead of DC [42,47].

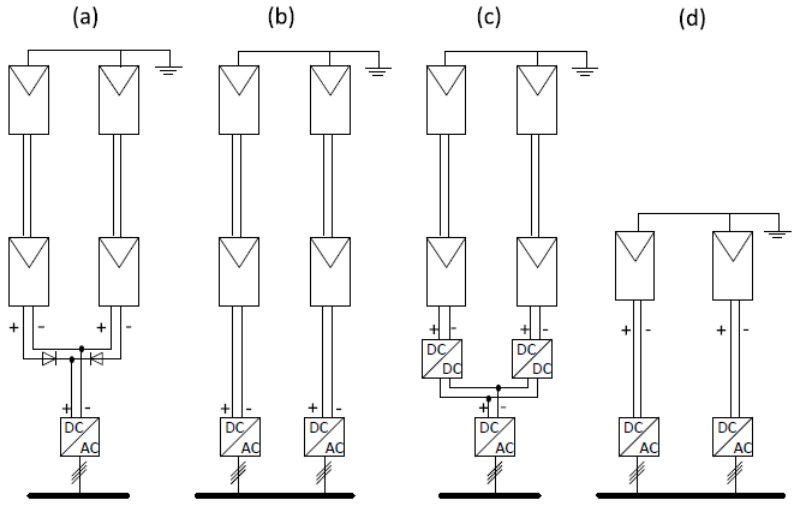

Figure 3.18.: PV inverter topologies. (a) Central, (b) String, (c) Multistring, (d) Module integrated [48].

3.3.2. Inverter comparison

After having reviewed the main types of inverters used in PV applications and based on Figure 3.19 it can be concluded that although the module integrated inverter is more reliable, flexible and offers a good range of efficiencies, its main disadvantage is the cost, while central inverters offer reasonable characteristics with few disadvantages, for this reason central inverters are the most common type in PV installations. Finally, it is worth-mentioning that the inverter must allow the PV module to continuously operate at the maximum power point (MPP) according to the maximum power point tracking (MPPT).

3.3.3. Efficiency of inverters

In an ideal case, all generated power by the PV system should be directly used for the loads or fed into the electric grid, however due to losses in the system this ideal scenario is rather unachievable. These losses result, for instance, from non-ideal properties that

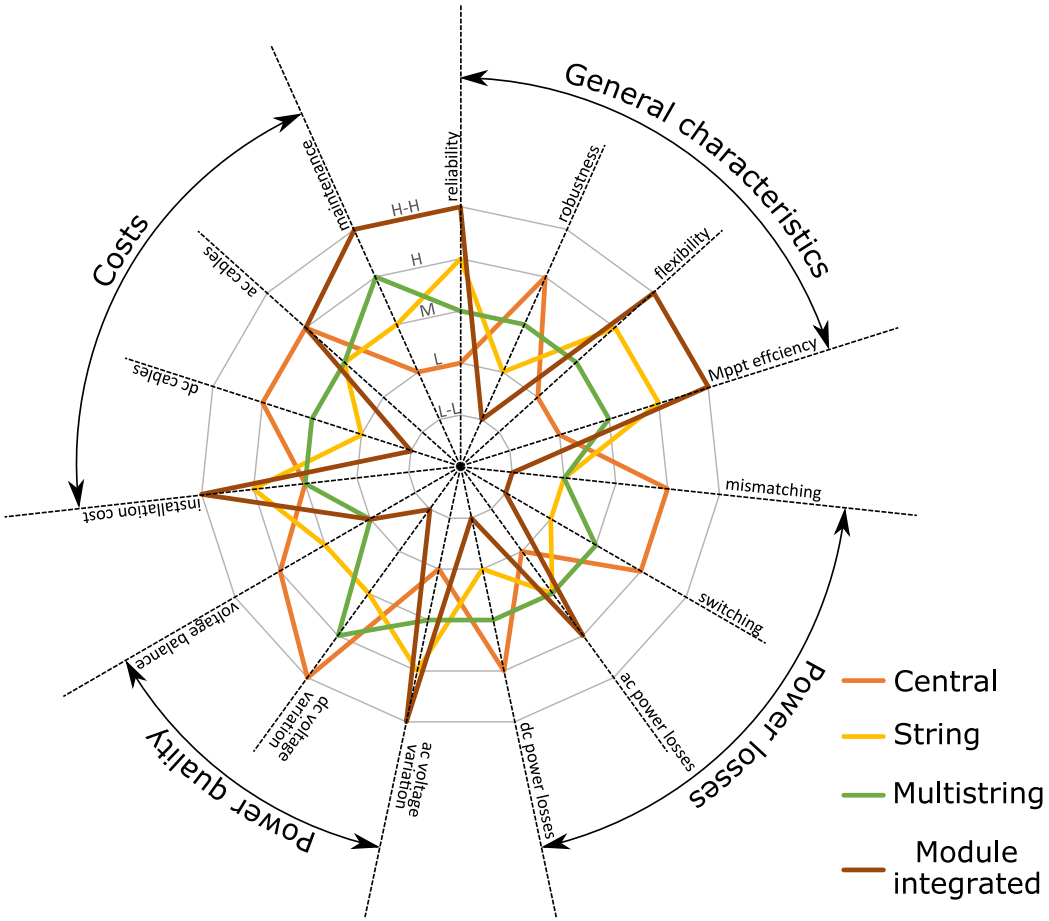

Figure 3.19.: PV inverter topologies comparison [48]

each real component has (i.e. heat losses caused by an ohmic resistance and inductance, as well as the switching losses in the semiconductors or during stand-by, some portion of power is consumed to keep the inverter powered), or the losses in the power part of the device itself [49].

3.3.3.1. Conversion efficiency

The conversion efficiency η_{con} is defined as the ratio between the DC power delivered by the solar generator and the AC power delivered to the AC loads or the AC grid, in other words, how much DC power is converted to AC power

$$\eta_{\text{con}} = \frac{P_{\text{AC}}}{P_{\text{DC}}}, \tag{3.32}$$

where P_{AC} is the inverter's output alternating current power and P_{DC} the inverter's input direct current power.

Over the last years the efficiencies of PV inverters have been improving continuously and further improvements are expected. For instance, new materials of the power components, e.g. silicon-carbide SiC, have proven to be able to reduce the losses. The bandgap of the SiC is very big (3.2 eV), causing a small intrinsic carrier concentration even for high temperatures. While transistors made out of silicon are used at approximately 150 °C, SiC's critical temperature is twice this value, hence making it possible to reduce the size of the heatsinks. Further advantages include, high possible reverse voltages, low forward resistances and reduced switching losses. Additionally SiC, allows high switching frequencies, thus smaller choke coils. However, as it can be expected SiC transistors are much more expensive than Si transistors, but what makes them competitive is their high inverter efficiencies, the first prototypes have shown peak efficiencies of 99% [49, 50]. Figure 3.20 depicts typical efficiency inverter curves, which were constructed using Table 3.3.

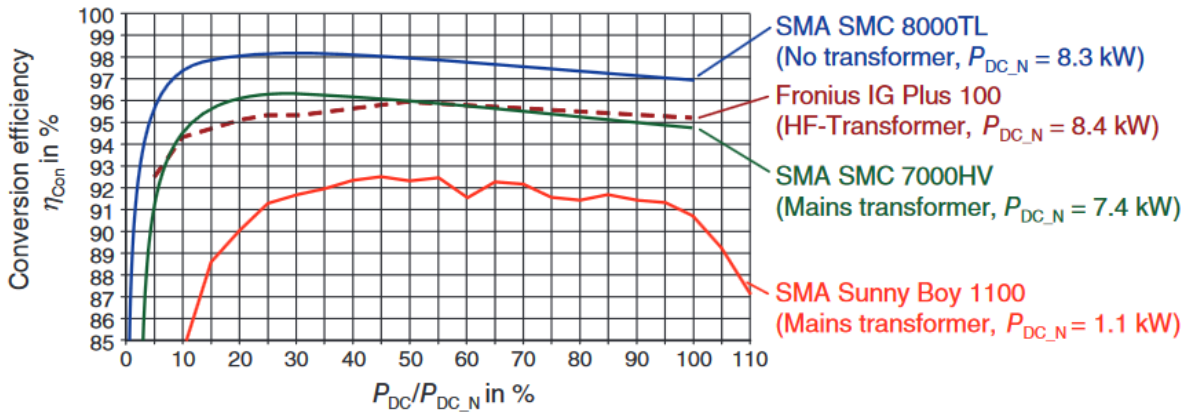

Figure 3.20.: Conversion efficiency η_{con} of different types of inverters: Clearly visible types with high frequency transformers and especially systems without transformers show the highest efficiencies [49].

Table 3.3.: Data for various types of inverters. [49]

Designation	Sunny Boy 1100	SMC 7000 HV	SMC 8000TL	SolarMax 6000S	IG Plus 100	Sunny Boy 5000TL	TLX 12.5k
Producer	SMA Solar Techn. AG	SMA Solar Techn. AG	SMA Solar Techn. AG	Sputnik Engin. AG	Fronious Int. GmbH	SMA Solar Techn. AG	Danfoss Drives AS
DC nom. power (kW)	1.1	7.35	8.25	5.3	8.42	4.83	12.9
AC nom. power (kW)	1	6.65	8	4.6	8	4.6	12.5
DC nom. voltage (V)	180	340	350	400	390	520	700
MPP region (V)	139-320	335-560	333-500	100-550	230-500	125-750	430-800
DC nom. current (A)	6.1	21.5	25	12	21.05	9	12
Max. efficiency (%)	93	96.2	98	97	96	95.5	98
Europe efficiency (%)	91.6	95.5	97.7	96.2	95.5	94.5	97.3
Number of inputs	2	4	4	3	6	3	3
Number of MPP-trackers	1	1	1	1	1	3	3
Feed-in	Single phase	Single phase	Single phase	Single phase	Single phase	Single phase	Three phase
Remarks	Mains transformer	Mains transformer	No transformer	No transformer	HF transformer	No transformer, multistring	No transformer, multistring

3.4. Control strategies currently used in PV systems

The integration of PV systems with battery storage systems into the power grid is an important aspect especially when introducing and talking about future energy concepts, like renewable energy. Using battery storage systems the amount of self-consumed electricity can be increased and the additional difference between the purchased remaining energy and generation costs can be used to finance the storage system.

Decent control strategies or modes of operation with positive effects on the power grid should be identified in order to quantify the potential benefits of having a PV-storage system. According to literature there are several control or operational strategies, in this work, only a few selected ones will be mentioned, in an attempt to give the reader an idea of what these control strategies are.

Note that only literature review has been carried out regarding some of the used control strategies in PV systems, some of which need to be modified when implementing the empiric part for future work in order to be applied in the system presented in this work.

3.4.1. Conventional (greedy) control strategy

This type of control strategy charges the battery whenever there is a surplus from the PV generator. This control strategy, is characterized for maximizing the self-consumption. Nowadays, EES applied in private households are usually operated in a way to maximize the self-consumption. The generated power is used to, preferably, satisfy the load demand and the excess power is then stored in the battery (which increases the self-consumption).

The battery control strategy which maximizes self-consumption transfers all power exceeding local demand into the battery, this way the battery is charged as early as possible in the day with the highest power (see Figure 3.21).

Therefore the utilization of the battery is maximal and the purchased energy from the power supply system is minimal.

In one hand, the smaller the PV system in a given household the bigger the fraction of energy which is instantaneously consumed, i.e. the higher the self-consumption. While on the other hand, increasing battery capacity leads to higher self-consumption rates. However, the bigger the storage capacity the smaller the relative gain in self-consumption [51].

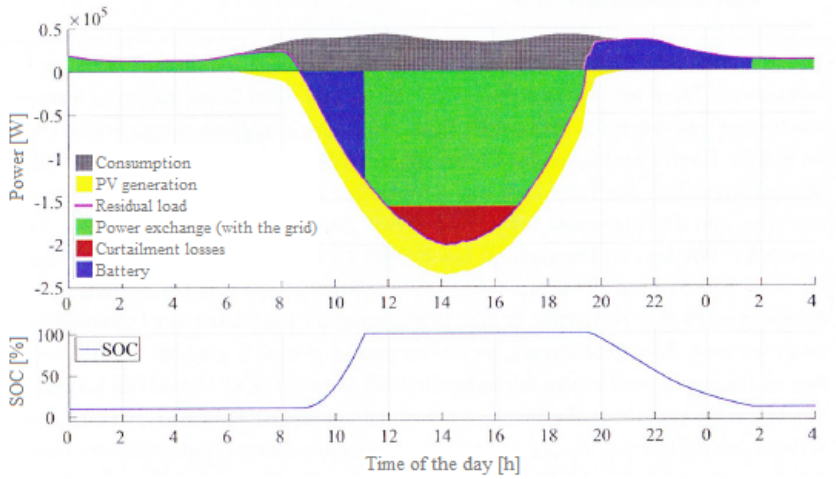

Figure 3.21.: Example of a simulation of a PV system with battery with the greedy control strategy [52].

3.4.2. Optimum self-consumption avoiding curtailment losses

Its main goal is to optimize the self-consumption and minimize the curtailment[4] losses (e.g. losses of green energy and economic losses) by means of storing energy over the feed in limit, in case that the energy is not enough to charge the battery, it is taken from the beginning of the day. The advantage of solar power is that it is easier to take up because the demand is usually higher around the early afternoon, time of the day when most solar power is produced. This curtailment is performed typically when an operator or utility (Distribution System Operator (DSO) or Transmission System Operator (TSO)) directs a generator to reduce its output, as it was previously mentioned [54]. Like the greedy strategy, Self-consumption Ratio (SCR) and Curtailment Loss Ratio (CLR) are optimal and a maximum SOC is achieved after the charging cycle, as it can be seen in Figure 3.22.

3.4.3. Dynamic feed-in limit

This type of control strategy is calculated on a daily basis and not depending on the time of the day. Its main goal is to determine the feed in limit so that the battery is charged with the cut off energy (see Figure 3.23).

Since the battery is charged from the moment the pre-calculated limit is exceed the energy

[4]Curtailment is defined as a reduction in the generator's output from what it could actually produce given available wind or sunlight [53]

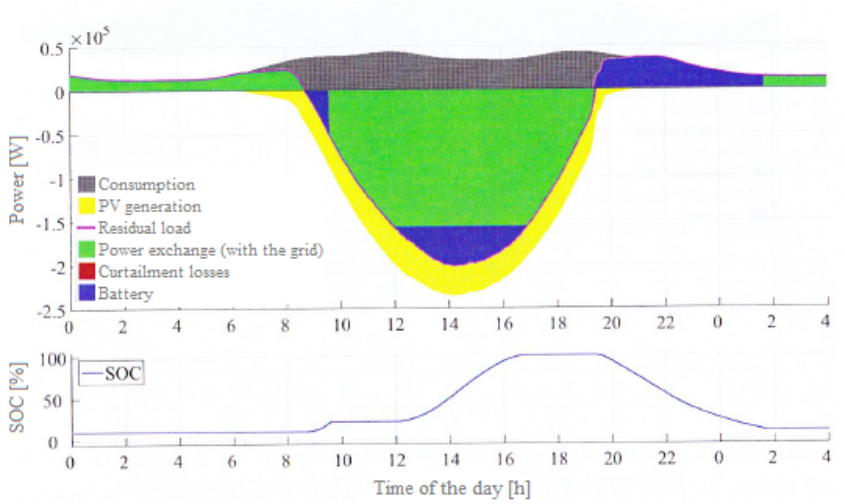

Figure 3.22.: Example of a simulation of a PV system with battery with optimum self-consumption avoiding curtailment losses control strategy [52].

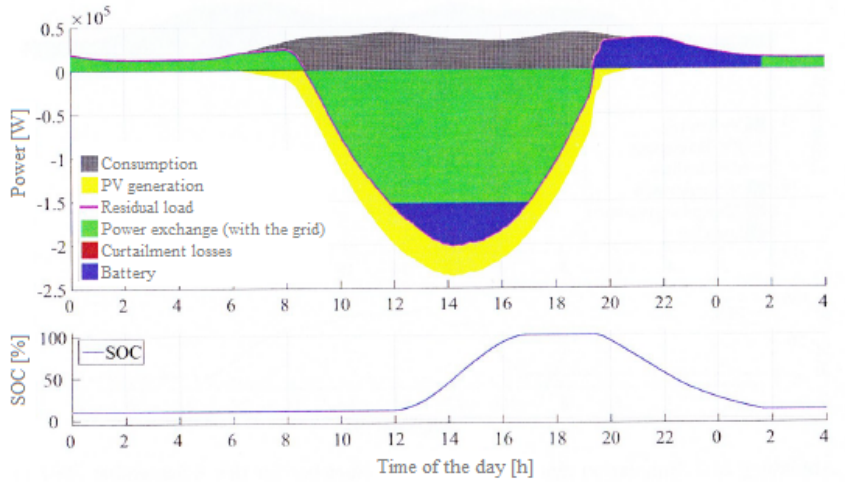

Figure 3.23.: Example of a simulation of a PV system with battery with the dynamic feed-in limit control strategy [52].

that is required by the loads cannot be taken from the battery. By using a dynamic limit an optimal SOC is guaranteed at the end of the charging cycle [52].

3.4.4. Dynamic feed-in limit with balancing

For this control strategy, the battery is charged based on the electricity price. Basically, when there is a high demand, the price also increases, while when there is an excess of electricity the price decreases. A limit is established and when this limit is passed then

the energy is stored (see Figure 3.24).

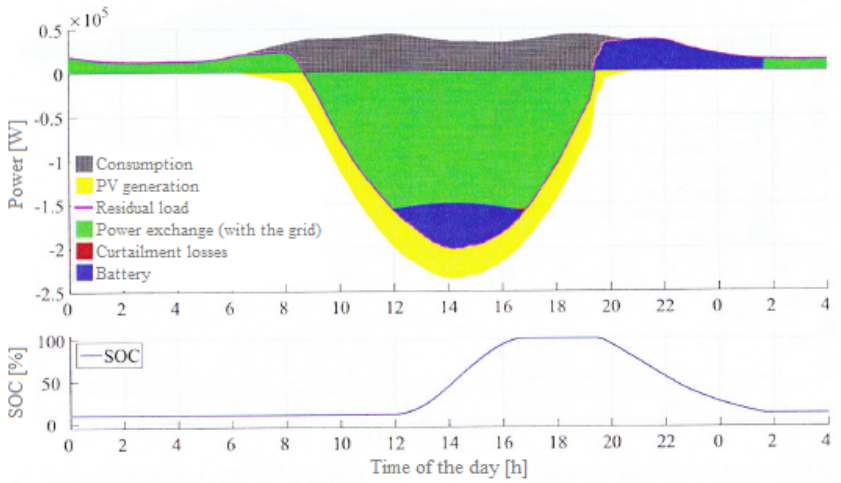

Figure 3.24.: Example of a simulation of a PV system with battery with the dynamic feed-in limit with balancing control strategy [52].

Likewise the previous control strategy, in this strategy an optimal SOC is guaranteed because the limit is dynamically calculated [52].

As it was aforementioned, some necessary changes should be implemented in presented control strategies (except for the conventional (greedy) one), these changes may include the post-ex view (having previously or existing data) or having a perfect weather prognosis.

4. Model description

Figure 4.1 shows an overview of the complete model that has been developed and is explained in this chapter, as it was previously mentioned the deployment of the model was carried out in MATLAB and Simulink.

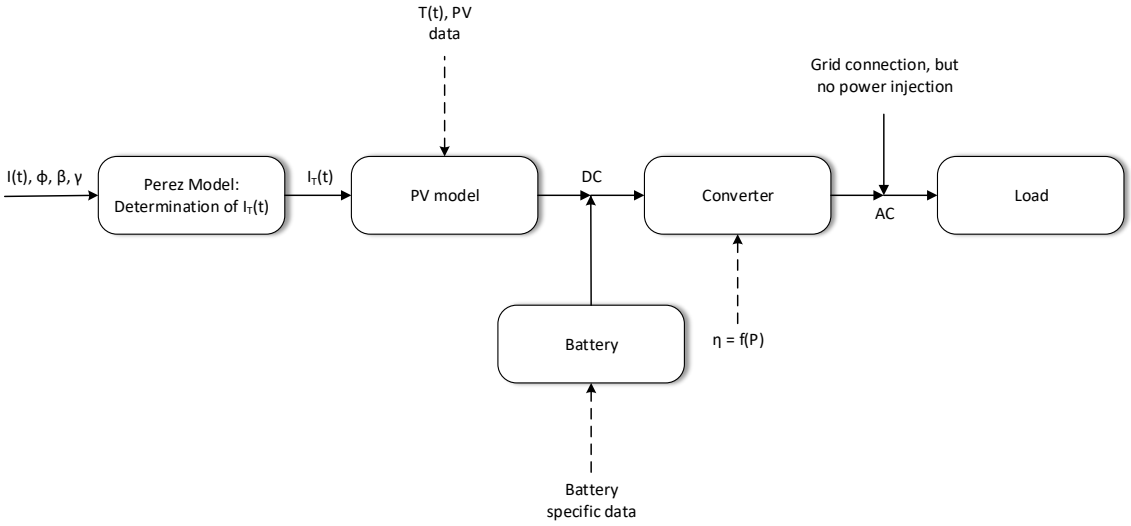

Figure 4.1.: Structure of the complete model.

It should be noted that 15 min timesteps are used for the simulation of the model and its standard input parameters are[1]:

- Surface's inclination β=30°
- Surface's orientation γ=0° (south oriented)
- Area=2.5 m^2
- Inverter's maximum power=500 W

[1]Note that the area, inverter's power and battery's capacity are actual data used in the initial setup given and used by the start-up company

- Maximum usable battery's capacity (i.e. state of charge) =960 Wh
- Battery's maximum output power=500 W
- Battery's efficiency=95 %
- Depth of discharge (DOD)=80 %

In the following sections, a description of each of the elements that comprise the PV system, moreover operational modes are presented.

4.1. PV and Perez model

As discussed in Section 3.1, three forms of modeling a PV module were introduced, but it was pointed out that the third one was the most accurate of them all and the one that resembled and simulated the behavior of a real PV module best. In this first part of the chapter, the developed PV model will be presented and explained. The selected software for this first model was Simulink, due to its ease of use and understanding. Note that the presented model is based on the model suggested by [18].

Firstly, the input parameters for the PV model must be defined. Yearly parameters, such as radiation and temperature where obtained from the Central Institute for Meteorology and Geodynamics ZAMG [2] in Austria. Figure 4.2 summarizes these parameters.

Furthermore these two parameters have to go through the Perez model[3] (a more sophisticated model requiring well measured data) in order to calculate the irradiance in a tilted surface, as was previously explained in Chapter 3.

Afterwards, the model of the PV module was deployed, using the model developed by [18] as a starting point. Table 4.1 lists the main parameters that are also required as input data of the Simulink model. Furthermore Figure 4.3 depicts a presentation of how the PV model looks at first hand, the two input parameters on the right side and the output current, voltage and power, as well as the possibility to plot the I-V and P-V characteristic curves of a PV module (on the left side can be seen the aforementioned Figure).

[2]By its abbreviations in German Zentralanstalt für Meteorologie und Geodynamik
[3]Based on the work and code presented in [55]

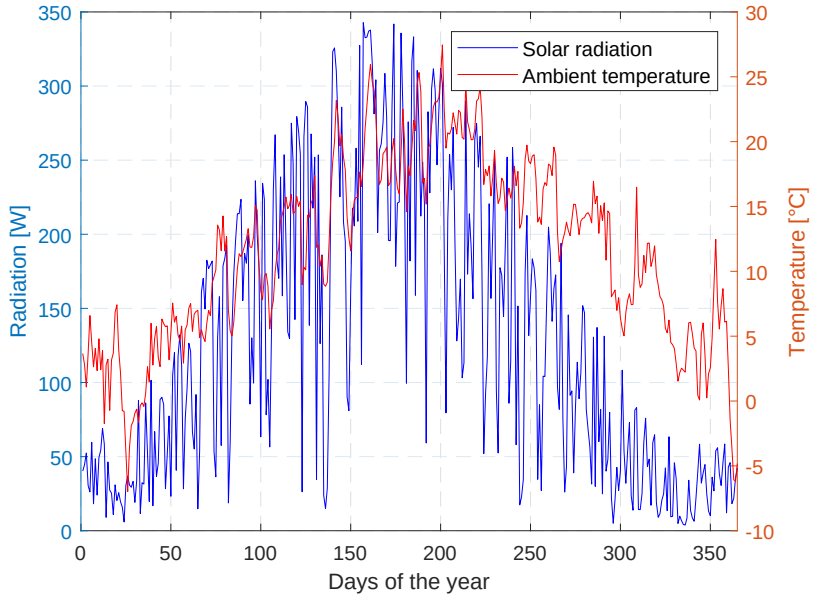

Figure 4.2.: Comparison of the yearly radiation with the ambient temperature evolution.

Table 4.1.: Main parameters of the PV module "10-02 Semiflex", which are the same that will be used for modeling it.

Parameter	Value
Temperature [°C]	24.80
V_{oc} [V]	22.60
I_{sc} [A]	5.35
P_{mpp} [W]	91.32
V_{mpp} [V]	18.33
I_{mpp} [A]	4.98
η_{module} [%]	13.34
η_{cells} [%]	16.54
Fill Factor (FF)	75.55

The advantage of Simulink is the way in which subsystems can be constructed within the main system, making it more organized and easier to understand and to follow the logic behind the model and its comprised mathematical equations. Additionally, it can be noticed that each subsystem can be easily connected to each other, and the output of

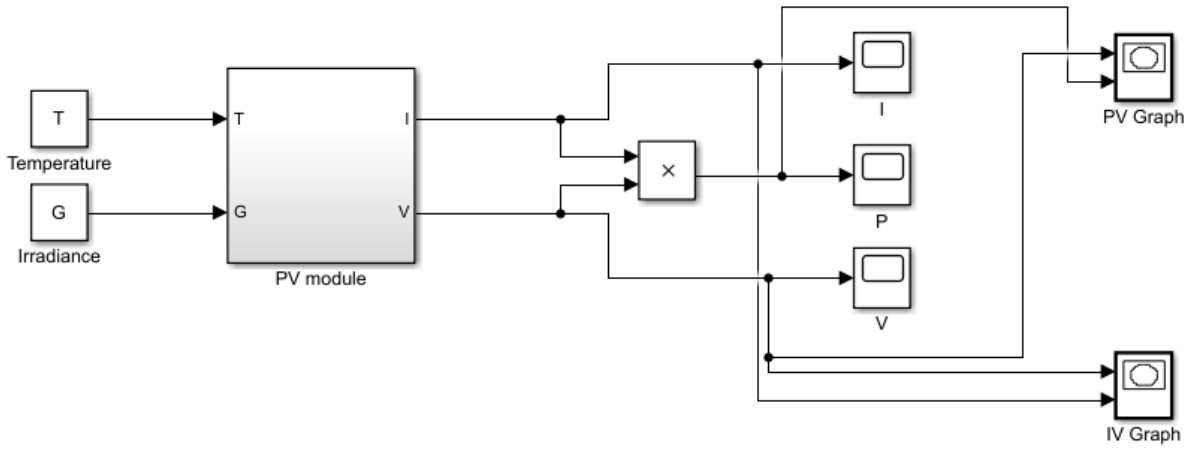

Figure 4.3.: The model's main mask, on the left side the two input parameters: temperature and irradiance and on the right the output parameters (current, voltage and power) and the characteristic curves.

one results in the input of another. It can be seen in Figure 4.4, that the PV module box (seen in Figure 4.3) is conformed by four subsystems. To ease the reader's understading, the blocks inside this subsystem are counted from left to right, i.e. $I_{o,ref}$ is block 1, I_o block 2 and so on.

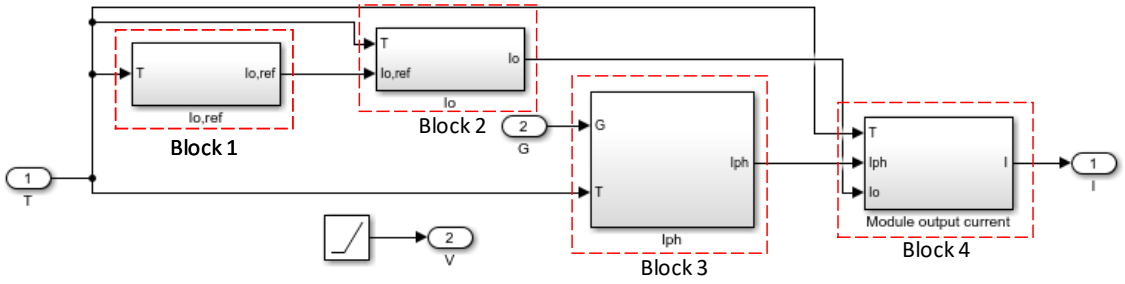

Figure 4.4.: Subsystems layout, view inside the PV module box.

Once again, it is possible to go one level deeper inside one of the subsystems shown in Figure 4.4. Next, the calculation of the reference diode saturation current $I_{\mathrm{o,ref}}$ will be performed as a first step (c.f. Figure 4.5). $I_{\mathrm{o,ref}}$ can be calculated using

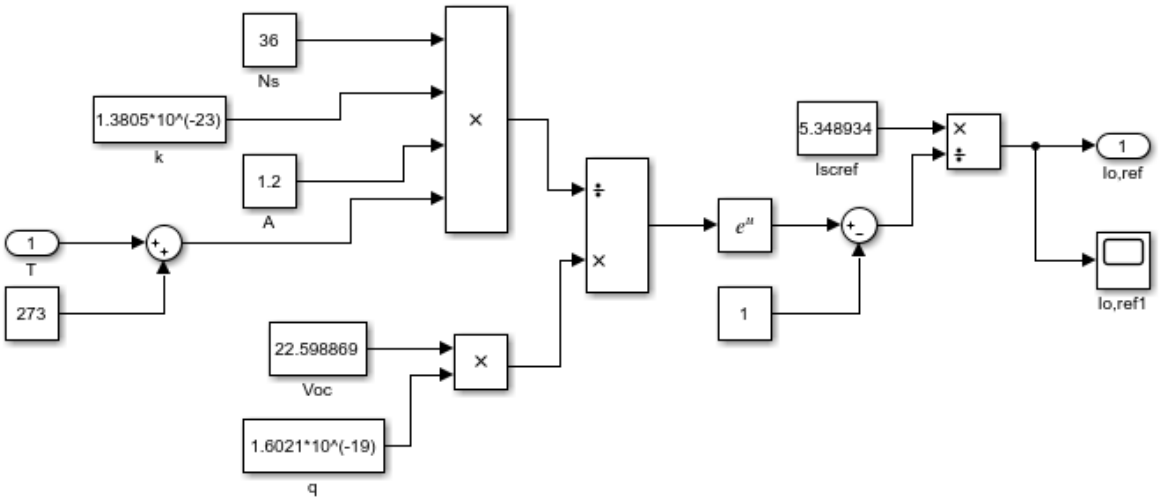

Figure 4.5.: Sub-subsystem containing the reference diode saturation current calculation $I_{\mathrm{o,ref}}$ (Block 1 in Figure 4.4).

$$I_{\mathrm{o,ref}} = I_{\mathrm{sc,ref}} \exp \cdot \left(\frac{-V_{\mathrm{oc,ref}}}{a} \right) , \tag{4.1}$$

$$a = \frac{N_{\mathrm{s}} \cdot A \cdot k \cdot T_{\mathrm{c}}}{q} , \tag{4.2}$$

where $I_{\mathrm{sc,ref}}$ and $V_{\mathrm{oc,ref}}$ are the short circuit current and open circuit voltage at STC [4], respectively. N_{s} represents the number of cells in series of the PV module, T_{c} the cell temperature, k and q are the Boltzmann and the electron constants (respectively), A is the ideality factor and a the modified ideality factor. Later on, this reference diode saturation current (also known as dark current) will serve, together with the temperature, as inputs of the next sub-subsystem.

Following with the next sub-subsystem, depicted in Figure 4.6, the diode saturation current is calculated using

$$I_{\mathrm{o}} = I_{\mathrm{sc,ref}} \exp \left(\frac{-V_{\mathrm{oc,ref}}}{a} \right) \cdot \left(\frac{T_{\mathrm{c}}}{T_{\mathrm{c,ref}}} \right)^3 \cdot \exp \left[\left(\frac{q \cdot \epsilon_{\mathrm{g}}}{A \cdot k} \right) \cdot \left(\frac{1}{T_{\mathrm{c,ref}}} - \frac{1}{T_{\mathrm{c}}} \right) \right] , \tag{4.3}$$

[4] By their English abbreviations Standard Test Conditions, that is a cell temperature of 25 °C and an irradiance of 1000 W/m^2, with an air mass of 1.5 (AM1.5)

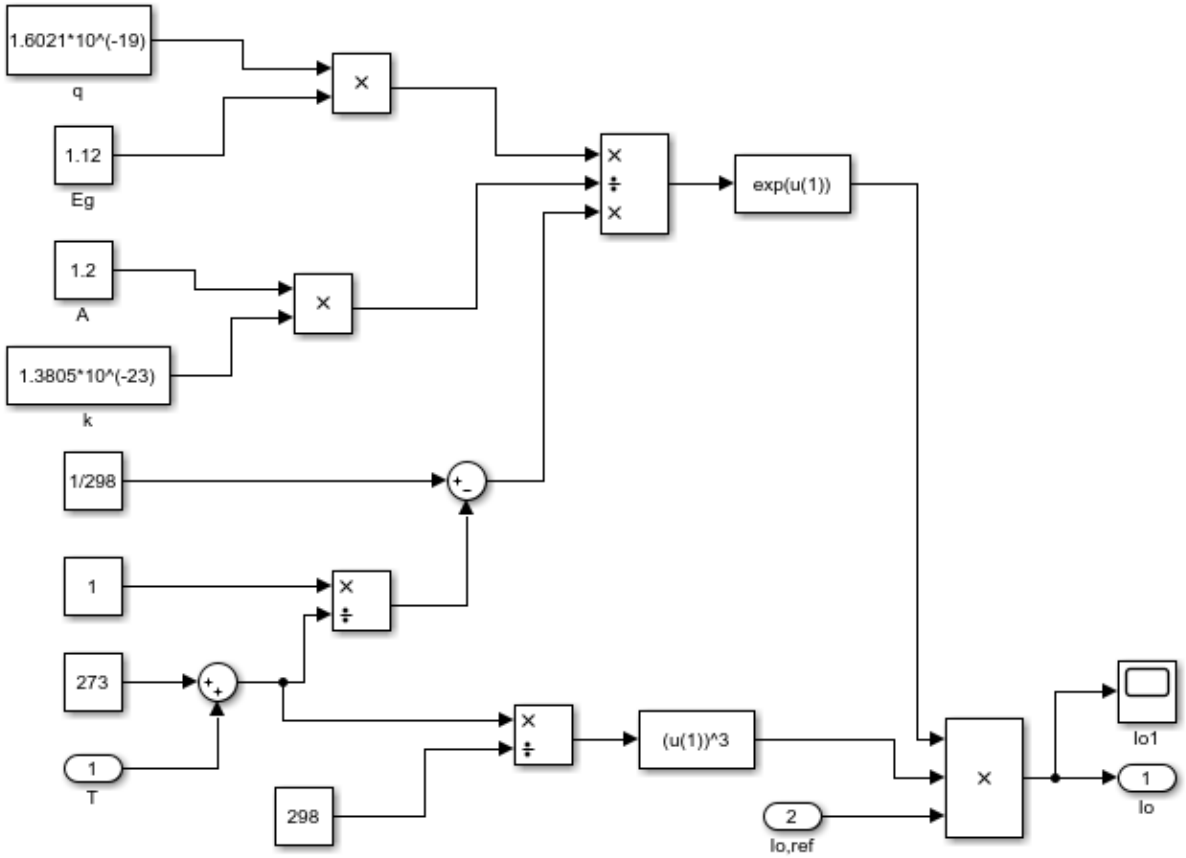

Figure 4.6.: Sub-subsystems calculating the diode saturation current calculation I_{o} (Block 2 in Figure 4.4).

where $T_{\mathrm{c,ref}}$ is the cell temperature at STC and ϵ_{g} is the material band gap energy[5]. The next sub-subsystem to be presented is the one that computes the photogenerated current, by utilizing

$$I_{\mathrm{ph}} = \frac{G}{G_{\mathrm{ref}}} \cdot (I_{\mathrm{ph,ref}} + k_{\mathrm{i}} \cdot \Delta T) \ , \tag{4.4}$$

where k_{i} is the short circuit current temperature coefficient, as at the time of conducting this work, no temperature coefficients were able to be provided due to the lack of them by the company who is interested in the current thesis. That being the case, in order to continue with development of the model, literature had to be consulted. A value of 0.0032

[5]Also known as the width of the band gap, it is the difference between the conduction energy and valence energy. For the case of Silicon the gap of energy equals to 1.12 eV, for Germanium 0.66 eV and Gallium Arsenide 1.45 eV to name a few examples.

A/K has been used from [19]. It should also be noted that a very common assumption in the modeling of PV devices has been made as presented in [18,19,56,57]

$$I_{\mathrm{sc,ref}} = I_{\mathrm{ph,ref}} \tag{4.5}$$

the reason behind this, is as previously mentioned in Chapter 3, practical PV devices present a low series resistance and a high parallel resistance. And so, after applying (4.5) in (4.4) results in

$$I_{\mathrm{ph}} = \frac{G}{G_{\mathrm{ref}}} \cdot \left(I_{\mathrm{sc,ref}} + k_{\mathrm{i}} \cdot \Delta T\right) , \tag{4.6}$$

which corresponds to what is shown in the Simulink sub-subsystem in Figure 4.7.

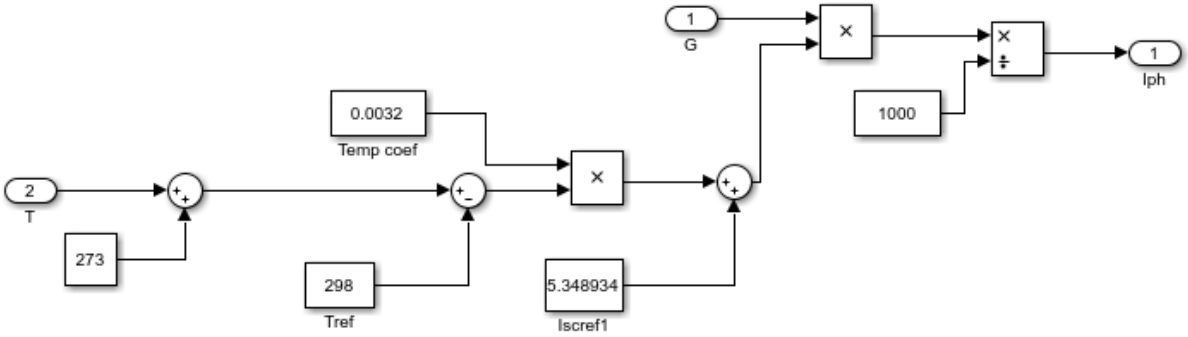

Figure 4.7.: Sub-subsystems containing the photogenerated current calculation I_{ph} (Block 3 in Figure 4.4).

Finally, the last subsystem can calculate the PV module's output current using the temperature, photogenerated and diode saturation currents provided by the previous subsystems. This is achieved by

$$I = I_{\mathrm{ph}} - I_{\mathrm{o}} \cdot \left[\exp\left(\frac{V + R_{\mathrm{s}} \cdot I}{a}\right) - 1\right] - \frac{V + R_{\mathrm{s}} \cdot I}{R_{\mathrm{p}}} , \tag{4.7}$$

where R_{s} and R_{p} correspond to the series and parallel resistances, respectively. Again, for this case, just like the temperature coefficient, their values had to be found in the literature, due to lack of information given by the start-up company in Graz. The values taken from [19] yield to values of 0.221 Ω for the series resistance and 415.405 Ω for the parallel resistances (c.f. Figure 4.8).

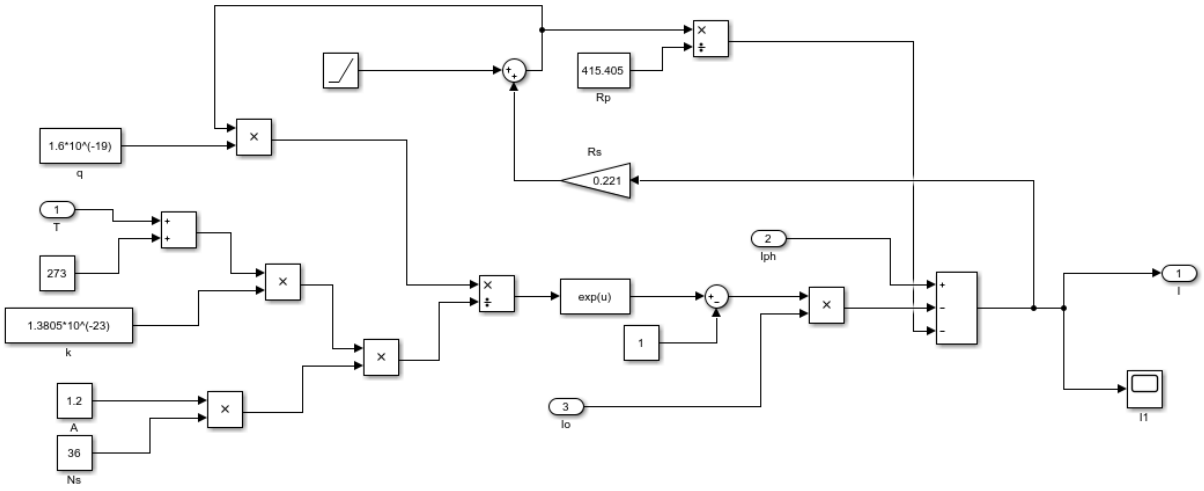

Figure 4.8.: Sub-subsystems containing the module's output current I (Block 4 in Figure 4.4).

4.1.1. Curve fitting equations in the PV model

During the development of the PV module, despite the ease and flexibility of Simulink, its major inconvenience are the speed limitations when handling big amounts of data. For that reason, using the results obtained from the Simulink model and by means of curve fitting, mathematical equations were developed in order to replicate the results of the results obtained with the Simulink model. A more detailed explanation of this subsection is presented in Chapter 5.

4.2. Battery model

A second very important component for the proposed PV system is the battery. As previously mentioned in Section 3.2, the utilized battery is a LIB (with a maximum output power of 500 W and an efficiency of 95 %), with one control strategy, based on four operation modes and a degradation model that includes the aging effect (dependent on the maximum DOD), in which the influence of the DOD over the SOC is analyzed. The idea behind the development of the battery model in MATLAB, is basically, to simulate it through power analysis and balances, and is going to be later on described and explained in Section 4.5.

4.2.1. Battery degradation model

Despite the steadily increasing lifetime of recently available lithium-ion batteries, the degradation of capacity and SOC of these batteries is still a big influencing parameter for the design and operation of battery energy storage systems. Therefore, the degradation process as a function of battery operations is critical. For this reason, a battery degradation model is integrated into the whole model, which estimates the battery's capacity fade and SOC decrease.

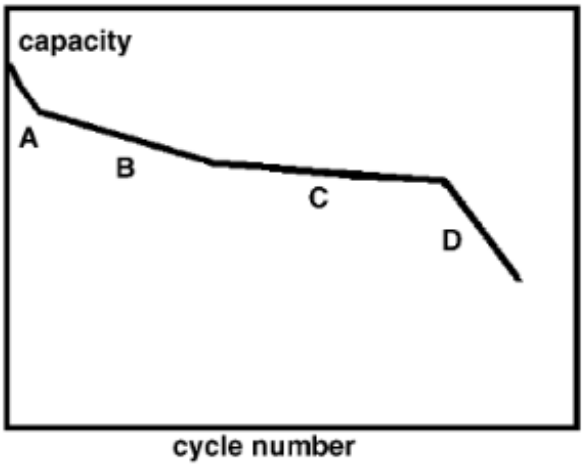

Figure 4.9.: Capacity degradation curve for a LIB [58].

The rate in which a battery is degradated not only depends on stress factors, like charging, discharging and time but also on its current state of life. Consequently, battery degradation is a non-linear process with respect to time and stress cycles, making it more difficult to have a predicting model of the aging process, it is for this reason that theoretical studies that include the DOD's influence to the amount of faded capacity are insufficient and so most of the models are empirical. These models based on degradation experiments are able to achieve an acceptable accuracy [59].

In Figure 4.9, a capacity degradation curve is depicted where four regions can be distinguished [58]:

- **Region A**, in which the rate in which the capacity decreases is high.
- **Region B**, the pace in which the capacity rate was decreasing in the previous region slows down.
- **Region C**, after some few hundreds cycles, the decrement in the capacity rate is

less abrupt.

- **Region D**, in this region the capacity rate decreases rapidly

The end of life of the battery occurs when the battery's capacity reaches 80% of its initial capacity, i.e. usually defined between regions C and D [58].

The degradation model that has been developed, consists of a series of degradation data measured experimentally from a well known battery manufacturer, whose inputs are the battery's number of cycles, the depth of discharge and the initial SOC.

4.2.2. Battery capacity and depth of discharge

Based on Figure 4.10, obtained from [60], mathematical equations were found, by means of using the curve fitting method, each of them for different values of depth of discharges. These equations have been implemented in the battery's model as a function, which calculates for each time step a new SOC, which, as expected, is decreasing with time. Detailed graphs (i.e. for DODs values from 10% to 100 %) with their corresponding mathematical equations are presented in the Appendix A (see Figure A.1a through Figure A.5b).

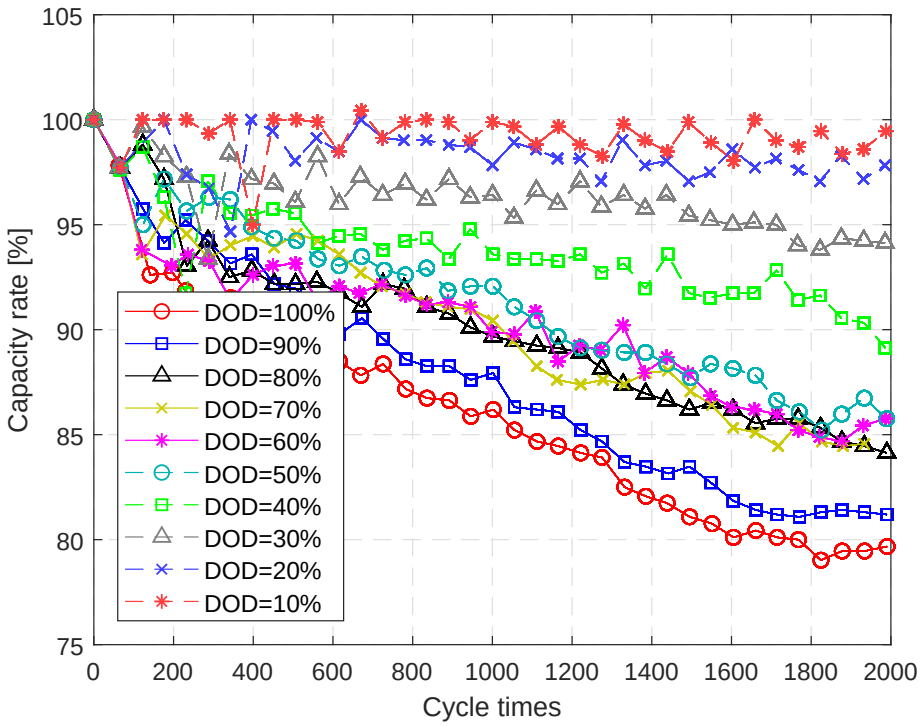

Figure 4.10.: Capacity rate at different cycles for different values of DOD.

4.3. Inverter model

A simple model has been developed, based on real measurements provided by the start-up in Graz, so that by means of curve fitting, two mathematical equations were found. Figure 4.11 shows the curve efficiency referred to the input power, that is, the power that goes into the inverter (left side of the inverter), i.e. the power produced by the PV module. This case is considered, for instance, when the PV power and the battery's power is not enough to supply the loads. While in Figure 4.12, the efficiency curve shown is referred to the output power, in this case the power that leaves the inverter (right side of the inverter), i.e. the actual power required by the loads.

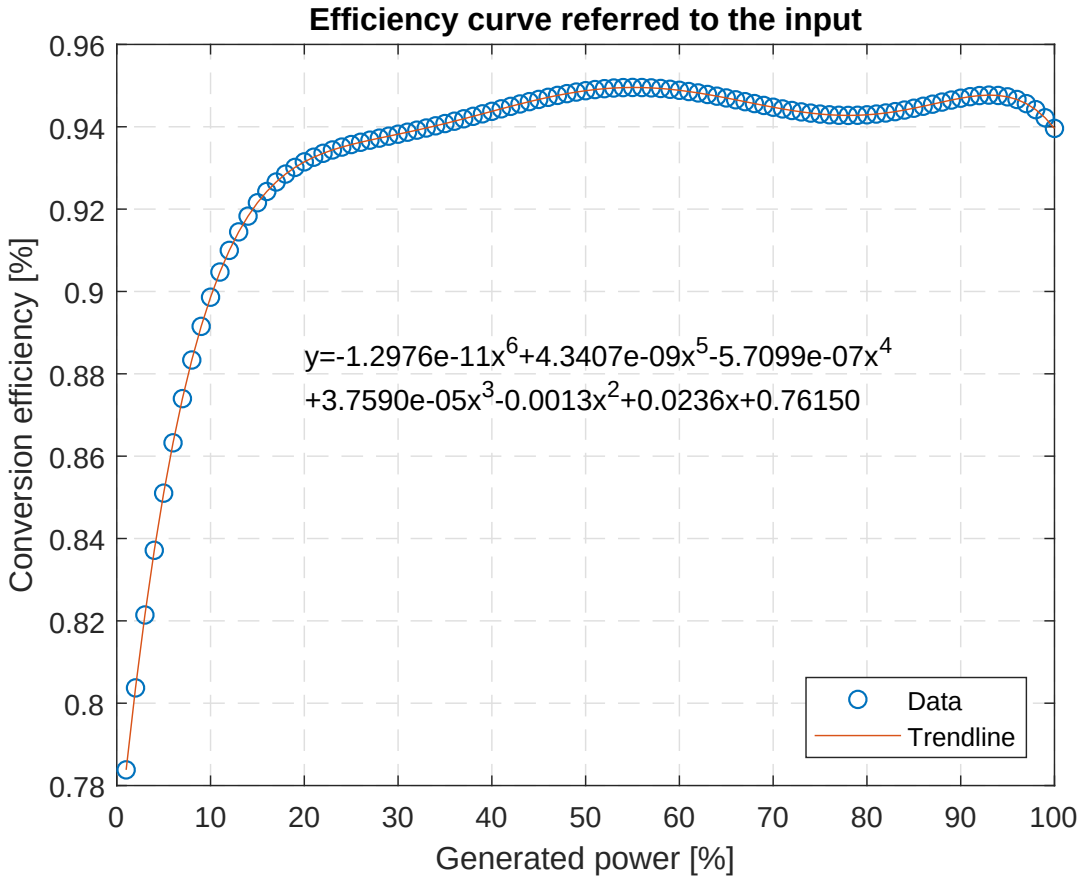

Figure 4.11.: Efficiency curve for the used inverter referred to the input power, constructed using real data (used in operational mode 4).

With the equations obtained with the curve fitting method the actual power fed into (or required by) the loads can be estimated by multiplying the actual power of the PV

generator (or the power required by the loads)[6] with the actual efficiency of the inverter, regardless of losses.

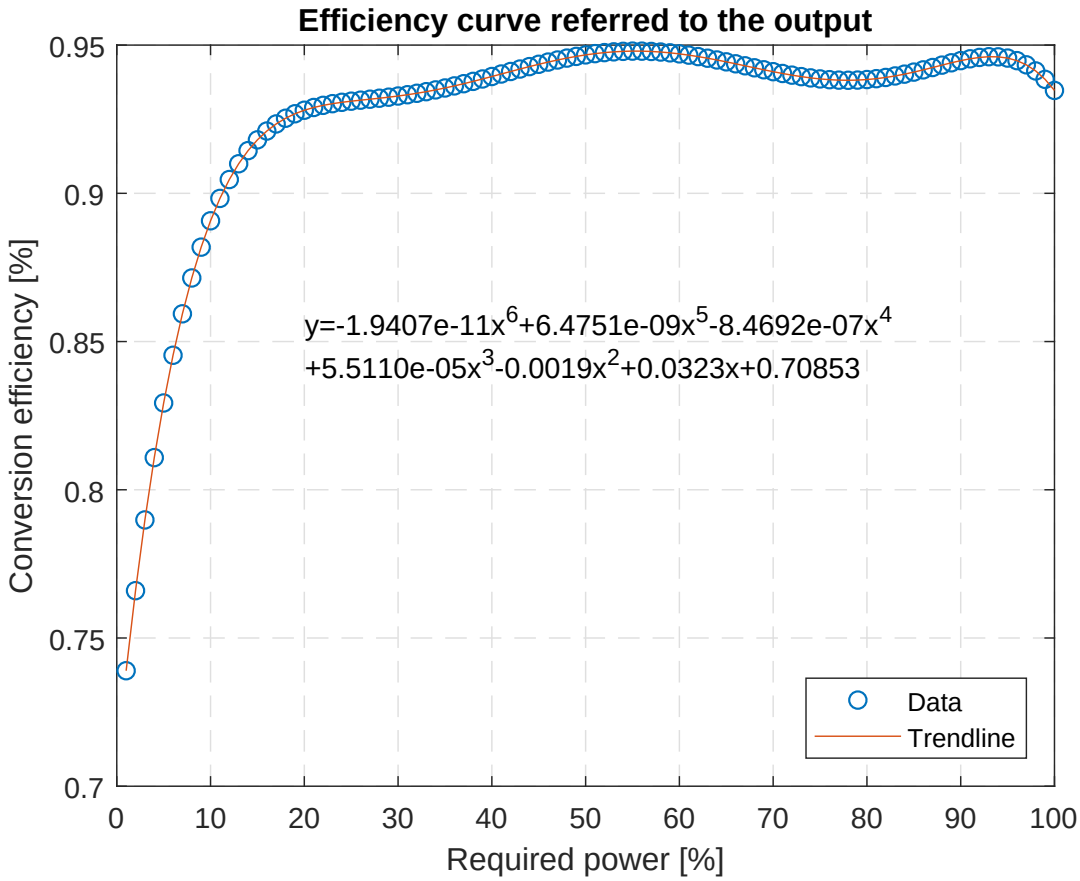

Figure 4.12.: Efficiency curve for the used inverter referred to the output power, constructed using real data (used in operational mode 1 and 2).

4.4. Load model

The load model is done based on a household's real data, provided by the university:

The data was measured in a three phase system, but an average value of all three phases was considered for this work.

In Figure 4.13, two periods where almost no power is consumed is seen, which are caused by holidays.

[6]Depending on the operational mode in which the battery is.

Table 4.2.: Used load parameters [61].

Parameter	Value
Load's energy [kW h]	960.98
Load's maximum power [W]	2657.7

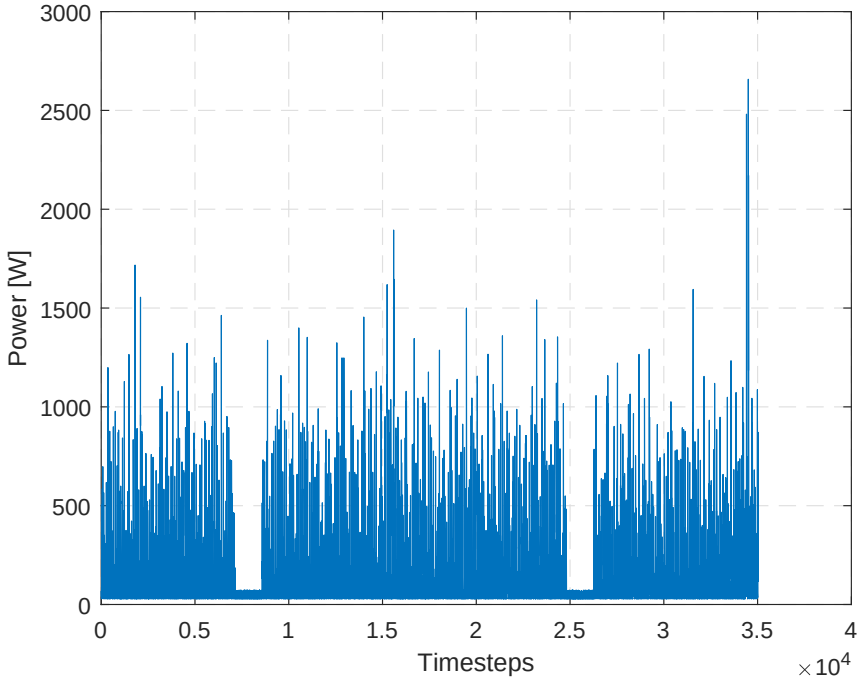

Figure 4.13.: Yearly load profile of a household, with two holiday periods (sections with almost no power).

4.5. Operational modes

In this subsection four operational modes are presented, depending on the amount of load needs, the generated PV power and the available power in the battery. A connection point with the grid exists, but only as a backup, energy injection to the grid is not possible in this system. Also notice that in the following figures that power can be either positive or negative, when the power enters or leaves the system, respectively.

Operation mode 1

The whole load can be supplied by the produced PV power, the excess of generated power goes directly to feed and charge the battery (see Figure 4.14), in order to fulfill this mode

the following conditions must be met:

$$P_{\text{pv}} < P_{\text{inv,max}} < P_{\text{load}}\,, \tag{4.8}$$

$$P_{\text{grid}} = 0\,, \tag{4.9}$$

$$P_{\text{battery}} \leq 0\,. \tag{4.10}$$

where P_{pv} is the power generated by the PV modules, P_{grid} is the purchased power from the grid and P_{battery} is the stored power in the battery. Note that P_{battery} is negative when the battery is being charged, and positive when being discharged. However, a case in which P_{grid} is different than zero can also occur if:

$$P_{\text{pv}} > P_{\text{inv,max}} > P_{\text{load}}\,, \tag{4.11}$$

$$P_{\text{grid}} = P_{\text{load}} - P_{\text{inv,max}}\,, \tag{4.12}$$

$$P_{\text{battery}} \leq 0\,. \tag{4.13}$$

This happens because the inverter's maximum power acts as a restrain, i.e. the power that goes into the inverter (generated power by the PV) is conditioned or limited by its maximum power, meaning that it cannot take anymore power than $P_{\text{inv,max}}$.

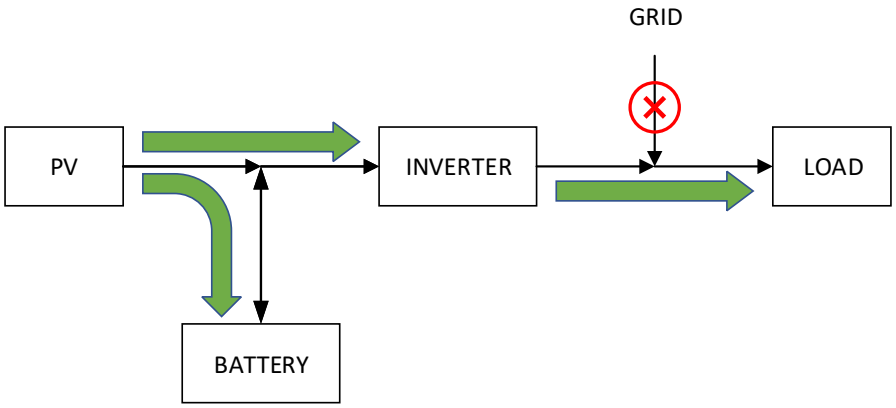

Figure 4.14.: Scheme of the operation mode 1 and its power flow

Operational mode 1, works as the greedy algorithm, described in Section 3.4. It is considered the most optimistic mode, because it is expected that the PV system is not only able

to fully supply the power demands but also have an excess of energy that is able to charge the battery. However, its drawback is that when the battery's charge level surpasses its maximum power, then the energy is not injected to the grid, hence the energy is lost.

Operation mode 2

In this operation mode, the generated power from the PV module is not enough to supply the loads, thus the stored energy inside the battery can help to fulfill the power requirements by the loads (see Figure 4.15), under the following conditions:

$$P_{\text{PV}} < P_{\text{load}} \leq P_{\text{PV}} + P_{\text{battery}}\,, \tag{4.14}$$

$$P_{\text{PV}} + P_{\text{battery}} < P_{\text{inv,max}}\,, \tag{4.15}$$

$$P_{\text{grid}} = 0\,, \tag{4.16}$$

$$P_{\text{battery}} > 0\,. \tag{4.17}$$

Likewise in Operation mode 1, P_{grid} can take a value different than zero when:

$$P_{\text{PV}} < P_{\text{load}} \leq P_{\text{PV}} + P_{\text{battery}}\,, \tag{4.18}$$

$$P_{\text{PV}} + P_{\text{battery}} > P_{\text{inv,max}}\,, \tag{4.19}$$

$$P_{\text{grid}} = 0\,, \tag{4.20}$$

$$P_{\text{battery}} > 0\,. \tag{4.21}$$

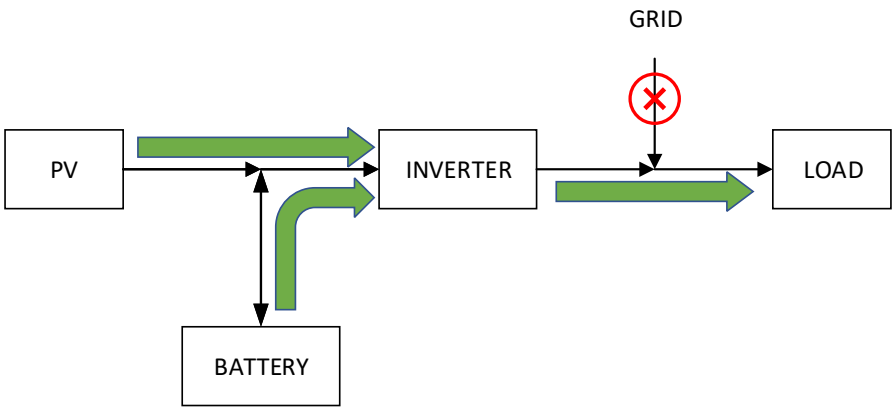

Figure 4.15.: Scheme of the operation mode 2 and its power flow

In this case scenario, there is no lost energy, but losses do exist at the inverter and during the battery's discharge.

For the aforementioned operational modes (i.e. mode 1 and 2), the inverter's efficiency is referred to the output, using the curve fitting equation shown in Figure 4.12.

Operation mode 3

This operation mode is the easiest to model, because in this case the loads cannot be supplied by neither the PV modules nor the battery, i.e. there is no sun and thus no energy generation and the battery has been emptied:

$$P_{\text{PV}} + P_{\text{battery}} = 0\,, \tag{4.22}$$

$$P_{\text{grid}} = P_{\text{load}}\,. \tag{4.23}$$

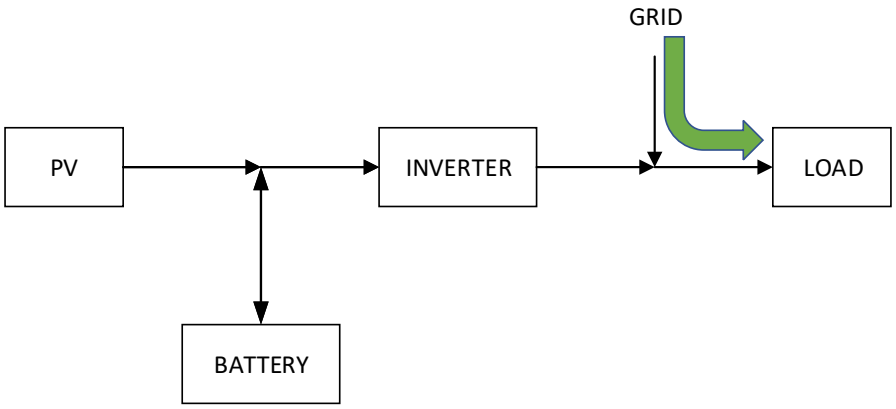

Figure 4.16.: Scheme of the operation mode 3 and its power flow

As seen in (4.23), the solution in case the condition in (4.22) is satisfied, therefore energy needs to be drained directly from the grid, as shown in Figure 4.16.

Operation mode 4

The fourth operation mode happens when the sum of the generated energy by the PV modules and the battery are still not enough to provide energy to supply the loads,

$$P_{\text{load}} > P_{\text{PV}} + P_{\text{battery}} > 0\,, \tag{4.24}$$

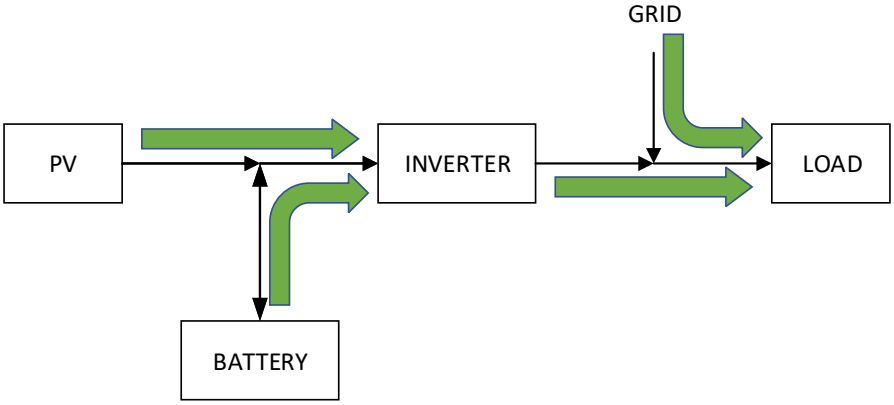

Figure 4.17.: Scheme of the operation mode 4 and its power flow

thus the remaining energy has to be taken from the grid (c.f. Figure 4.17), this time the calculation of inverter's efficiency is referred to the output following the curve fitting equation depicted in Figure 4.11

$$P_{\text{load}} = P_{\text{grid}} + P_{\text{inv,out}} \,, \tag{4.25}$$

$$P_{\text{inv,out}} = P_{\text{inv,in}} \cdot \eta_{\text{inv,in}} \,. \tag{4.26}$$

Where $\eta_{\text{inv,in}}$ is the inverter's efficiency referred to the input, moreover, replacing (4.26) in (4.25):

$$P_{\text{load}} = P_{\text{grid}} + P_{\text{inv,in}} \cdot \eta_{\text{inv,in}} \,, \tag{4.27}$$

$$P_{\text{inv,in}} = P_{\text{PV}} + P_{\text{battery}} \,, \tag{4.28}$$

$$P_{\text{load}} = P_{\text{grid}} + (P_{\text{PV}} + P_{\text{battery}}) \cdot \eta_{\text{inv,in}} \,. \tag{4.29}$$

Finally the power that is required by the loads is obtained by substituting (4.28) in (4.27).

4.6. Sensitivity analysis

For the sensitivity analysis, a sweep of the standard parameters (shown in Table 4.3) has been implemented over the ranges summarized in Table 4.4. This is done in order to de-

termine the influence that each parameter has over the whole system or, more specifically, over the saved energy.

Table 4.3.: Defined standard parameters.

Parameter	Value
PV module's inclination [°]	30
Surface orientation [°]	0
PV module area [m^2]	2.5
Maximum inverter power [W]	500
Battery's capacity [Wh]	960
Battery's maximum output power [W]	500
Battery's efficiency [%]	95

Table 4.4.: Variations of the standard parameters in order to perform the sensitivity analysis.

Parameter	Value	Increment
PV module's inclination [°]	0 to 90	1
Surface orientation [°]	-90 to +90	1
PV module area [m^2]	1.5 to 6	1.5
Maximum inverter power [W]	100 to 1000	100
Battery's capacity [Wh]	500 to 2500	100

5. Results and discussion

This chapter is devoted to present the most meaningful results regarding the overall model. At the same time a discussion about the obtained results is given, as well as an overview of the encountered problems and challenges along the work.

5.1. PV module's characteristic curves and MPP tracking

The PV module modeled in Simulink, previously discussed in Section 4.1, is able to generate the characteristic curves of a PV module, such as the current-voltage "I-V" and power-voltage "P-V" curves. For evaluating these two characteristic curves, two scenarios are considered:

1. The irradiance is varied from $0\,\mathrm{W/m^2}$ to $1000\,\mathrm{W/m^2}$ in increments of $200\,\mathrm{W/m^2}$, while maintaining a constant temperature of $25\,^{\circ}\mathrm{C}$.
2. The temperature is varied from $0\,^{\circ}\mathrm{C}$ to $60\,^{\circ}\mathrm{C}$ ($0\,^{\circ}\mathrm{C}$, $25\,^{\circ}\mathrm{C}$, $45\,^{\circ}\mathrm{C}$, $65\,^{\circ}\mathrm{C}$), while the irradiance is kept at a constant value of $1000\,\mathrm{W/m^2}$.

5.1.1. Results from the Simulink model

As can be observed in Figure 5.1a, with the increase in the irradiance the short circuit current increases extraordinarily, given that I_{sc} is linearly proportional to the irradiance over a wide range.

It can be observed that the open circuit voltage is low when the irradiance is low, however it should be noted that it increases logarithmically with the irradiance

$$V_{\mathrm{oc}} = \frac{A \cdot k \cdot T_{\mathrm{c}}}{q} \ln\left(\frac{I_{\mathrm{ph}}}{I\mathrm{o}} + 1\right) . \tag{5.1}$$

Note that higher irradiances mean higher photogenerated currents I_{ph} and thus the power is also increased (c.f. Figure 5.1b).

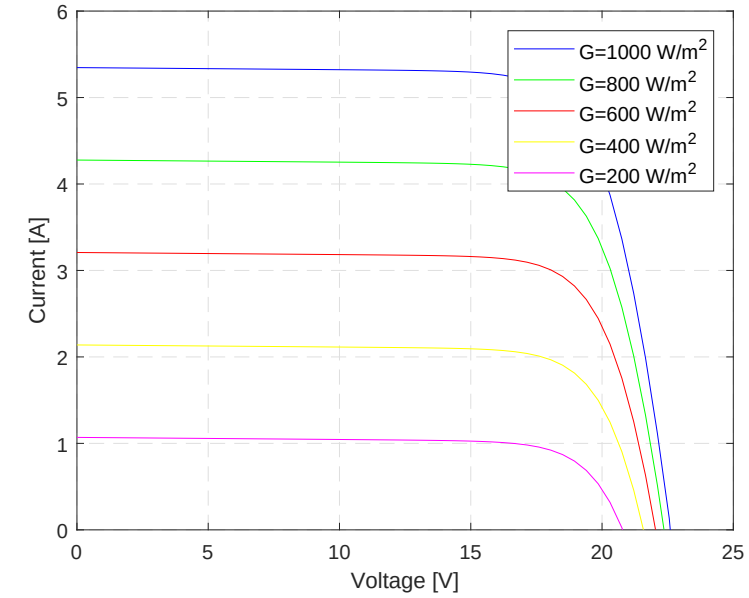

(a)

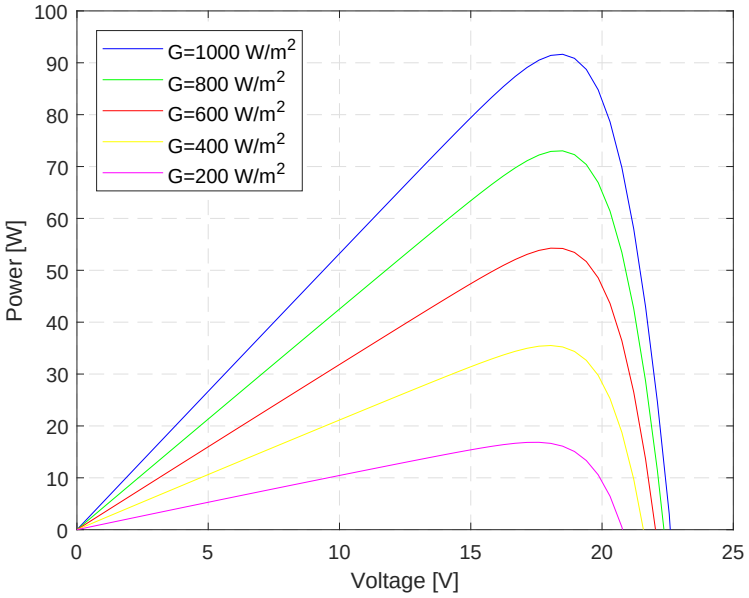

(b)

Figure 5.1.: (a) I-V curve plotted for different irradiances at 25 °C (b) P-V curve plotted for different irradiances at 25 °C.

Figure 5.2a shows that when increasing the temperature, a small increase in the short circuit current happens as well as a noticeable decrease in the open circuit voltage (c.f. Figure 5.2b).

The reasoning behind this, is explained with (5.2), further temperature effects are justified with (5.3) and (5.4).

$$I_{\mathrm{sc}} = I_{\mathrm{sc,ref}} \cdot \frac{G}{1000} + \alpha(T_{\mathrm{c}} - 25) \tag{5.2}$$

$$V_{\mathrm{oc}} = V_{\mathrm{oc,ref}} - \beta(T_{\mathrm{c}} - 25) + A \cdot V_{\mathrm{T}} \cdot \ln \frac{I_{\mathrm{sc}}}{I_{\mathrm{sc,ref}}} \tag{5.3}$$

$$\eta = \eta_{\mathrm{ref}}[1 - \delta(T_{\mathrm{c}} - 25)] \tag{5.4}$$

It is worth mentioning that I_{sc} increases slightly, around 0.07 %/°C, while the power and the efficiency decrease with the temperature in a range of 0.4 to 0.5 %/°C. It is important to highlight that the MPP is maintained at all times, this is important in order to obtain the maximum amount of power possible. At a specific time, a certain voltage level will result in a maximum power. Therefore, in this work, the maximum power and their corresponding current and voltage are calculated, by a simple implementation in a MATLAB, which finds the maximum values in each vector that contains the power, current and voltages and further on with help of the curve fitting (mentioned in Subsection 4.1.1 and presented in Subsection 5.1.3) to obtain mathematical equations that comprise the behavior of a PV module, and in this way is to be able to integrate it with the overall MATLAB script.

5.1.2. Challenges

Simulink – a graphical extension of MATLAB – is a very powerful tool for modeling and simulation of systems, specially nonlinear systems and due to its wide components library, many different applications and systems can be modeled. Despite all of that, during the elaboration of this work, an encountered problem was the duration of the simulation. Since a big amount of data is being handled (i.e. yearly irradiance data, load data, etc.), the simulations carried out in Simulink took a long time, however, a clever solution was to adopt the curve fitting method and thereby integrate it to the main MATLAB script. Another encountered challenge, was a certain amount of data (e.g. temperature

coefficients, parallel and series resistances, etc.) that was not provided and thus invoking to literature was the last resource.

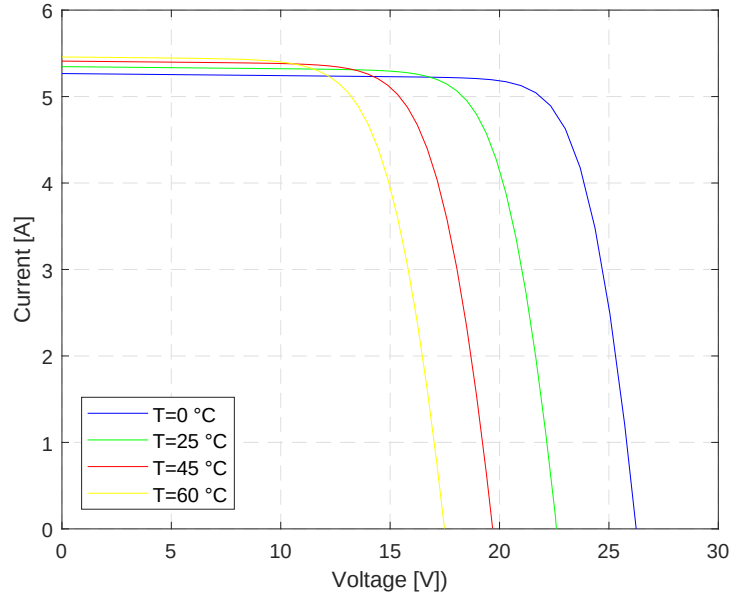

(a)

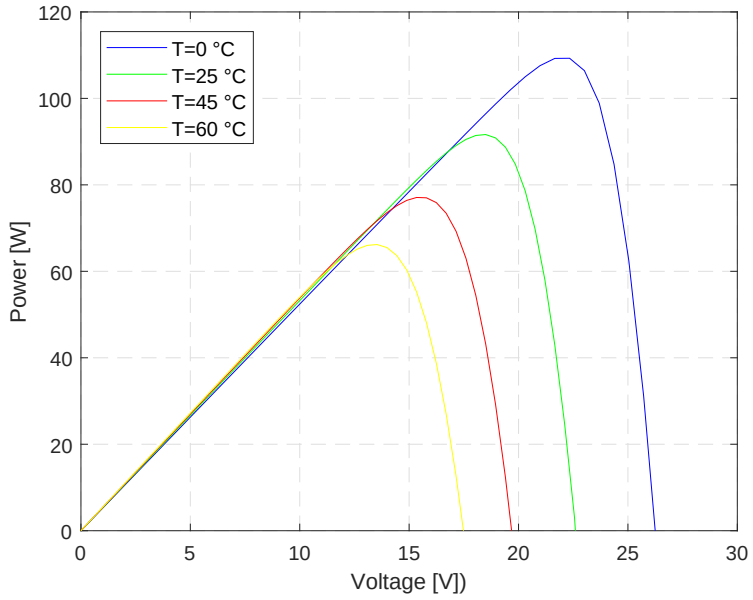

(b)

Figure 5.2.: (a) I-V curve plotted for different temperatures at 1000 W/m^2 (b) P-V curve plotted for different temperatures at 1000 W/m^2.

5.1.3. Results from the curve fitting of the PV model

As previously mentioned in Subsection 4.1.1, utilizing results from the Simulink PV model so that the simulation time is optimized, two mathematical equations were developed, one that is related to the irradiance and the second one related to the temperature (c.f. Figure 5.3 and Figure 5.4, respectively).

$$P_{\mathrm{PV}} = (3 \times 10^{-11} \cdot G^4 - 7.284 \times 10^{-8} \cdot G^3 + 6 \times 10^{-5} \cdot G^2 + 0.0744 \cdot G) \left[(-0.7225 \cdot T + 17.989) \cdot \frac{G}{1000}\right], \tag{5.5}$$

where P_{PV} is the generated power by the PV module, G is the irradiance received by the tilted surface and T represents the temperature on the PV module. Note the extra term at the end of (5.5), it is an scaling factor or correction term, its purpose is to scale or relate the second expression to the main expression (which is function of the irradiance). The reason behind this, is because the second expression was calculated at a constant irradiance ($1000\,\mathrm{W/m^2}$).

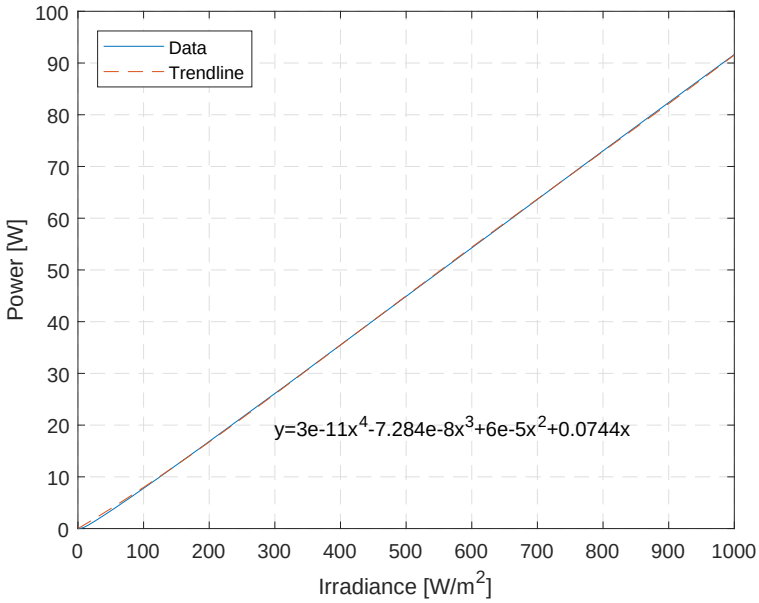

Figure 5.3.: Curve fitting when irradiance is varied and temperature is kept constant at 25 °C.

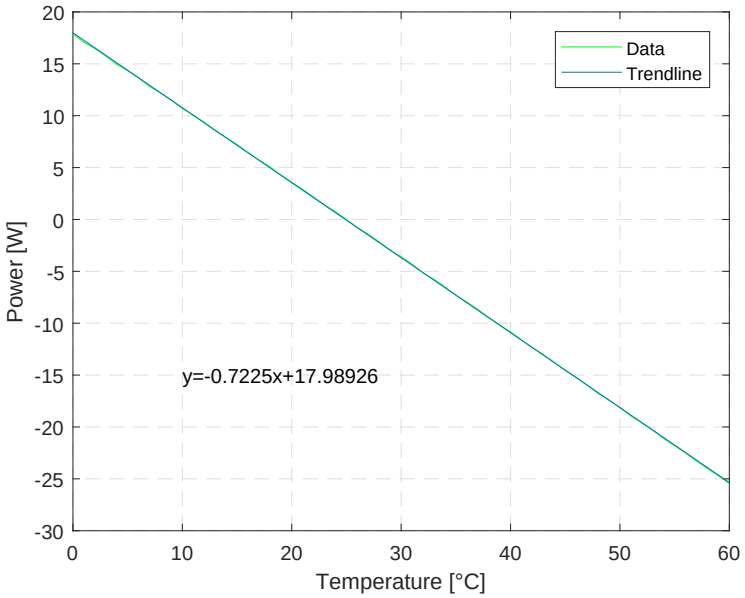

Figure 5.4.: Curve fitting when temperature is varied and irradiance is kept constant at $1000\,\mathrm{W/m^2}$.

5.2. Results from the sensitivity analysis and aging effects

This section presents the results obtained after performing a sensitivity analysis in the main system, as previously discussed in Section 4.6, a series of independent proposed parameters is varied to find out the impact on a particular dependent variable, which in this case is the saved energy, i.e. the energy that it does not need to be purchased from the grid, instead the loads can be either supplied by the PV system or by the battery.

The tilt angle and orientation play an important role in maximizing the solar radiation collected by a PV panel. Figure 5.5 show that a surface tilted on 30° and south oriented ($\gamma = 0°$) is the optimum position and orientation to demand the least amount of energy from the grid.

Moreover, as expected, the bigger the PV's area the more energy is generated and thus less energy is needed from the grid (c.f. Figure 5.6a). However, PV panels are developed in standardized sizes which are tightly related to the expected demand (the amount of energy required to provide all loads that are being supplied by the PV system).

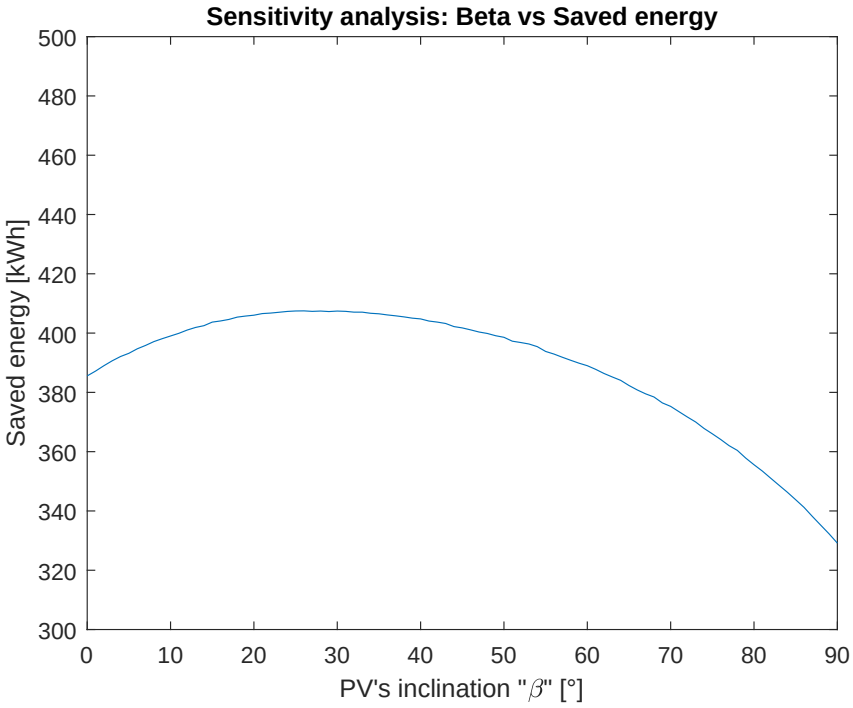

(a)

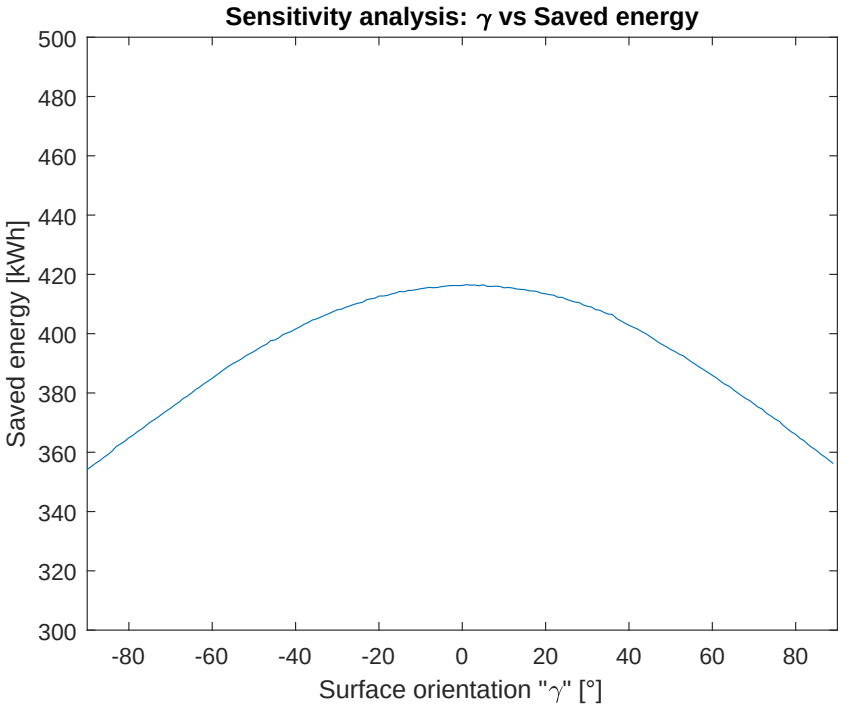

(b)

Figure 5.5.: Results from the sensitivity analysis (a) The PV's orientation "β" is being varied from 0° to 90° (b) The surface orientation "γ" is being varied from 0° to 90°.

The inverter, is a very important element in a PV system, its efficiency drives the efficiency of the PV system because their task is to convert DC (as produced by the solar panels) into AC (as consumed by most loads and the electric grid). Hence, the effect on the overall system if the inverter is oversized or undersized is an important factor to evaluate. As seen in Figure 5.6b, one can conclude that a bigger inverter brings better results in terms of the needed energy from the grid (saved energy).

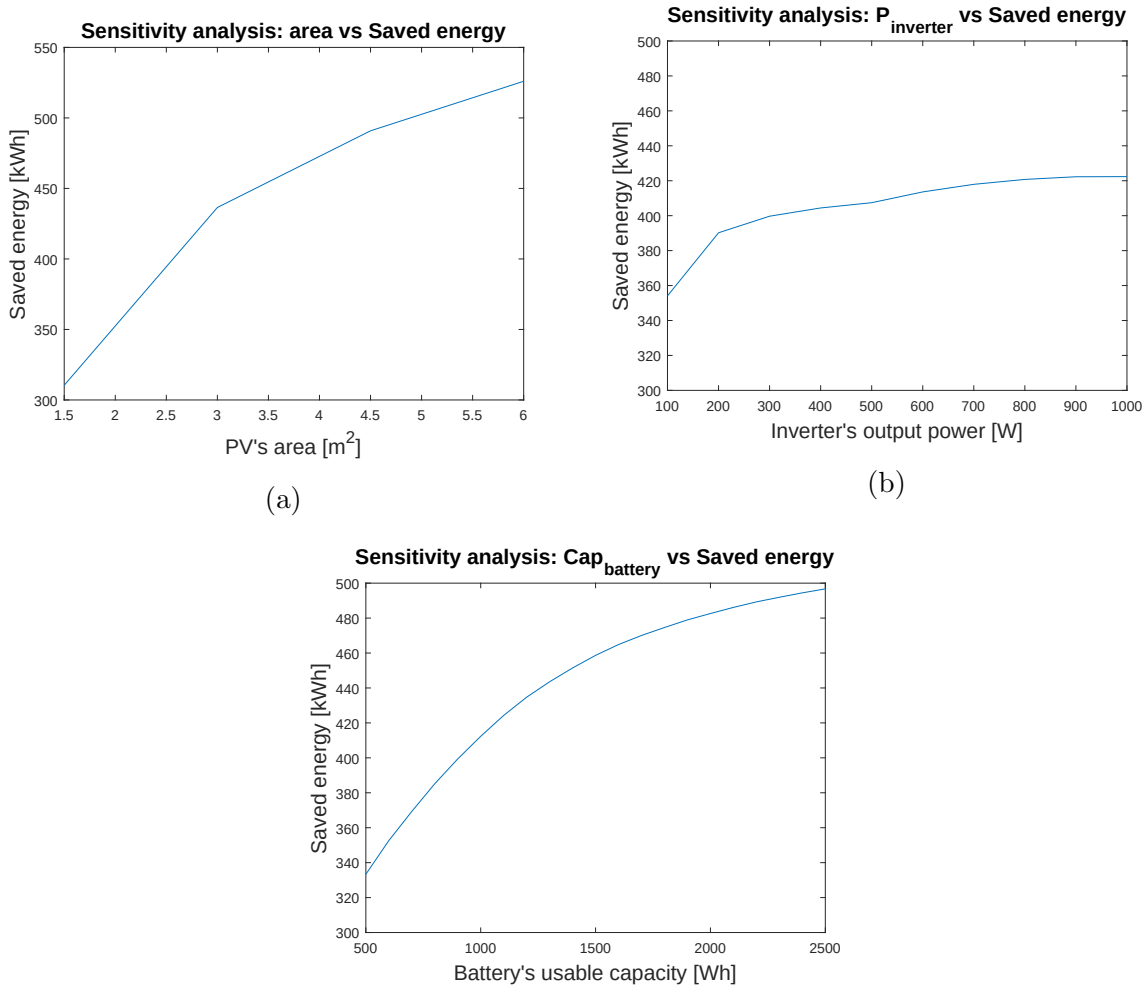

Figure 5.6.: Results from the sensitivity analysis (a) The PV's area is being varied from 1.5 m^2 to 6 m^2 (b) The inverter's output power is being varied from 100 W to 1000 W (c) The battery's usable capacity is being varied from 500 W to 2500 W, according to Table 4.4.

As it was seen in Figure 4.11 and Figure 4.12, the PV's inverter works optimally within a predetermined operational range (for instance, in the inverters used in the present work,

an efficiency less than about 94 % would be considered suboptimal). Depending on the power input coming from the PV panel, the inverter's efficiency to convert from DC to AC differs. Therefore, if the power input from the PV panel falls within this optimal range, then the inverter would work optimally.

Undersizing the inverter would mean that the maximum power output from the system would be defined and limited by the inverter, regardless of the amount of power generated from the PV panels, this power would be cut-off or limited by the inverter so that it does not exceed the inverter's rated capacity. A case like this would indeed be wise, in case of low amount of sunlight or irradiance on the PV panels either due to the location/climate or the orientation of the PV panel or other reasons.

On the other hand, oversizing the inverter, i.e. selecting an inverter whose maximum capacity is bigger than the nominal capacity of the PV panel, could be an option, for example, when thinking about increasing the number of PV panels. However, this could lead to overall lower efficiencies, even though inverters are usually designed to handle lower energy inputs than their nominal capacity, some limitations can arise.

The last parameter that was evaluated in this sensitivity analysis is the battery's capacity. This can be a very interesting parameter, because sizing the battery bank appropriately is a key factor in PV systems. The main goal when sizing the battery bank is that it is able to handle the generated power from the PV panels and provide enough stored power to the loads. Naturally, as it was expected, in Figure 5.6c, the bigger the battery the more energy saved, i.e. less energy needs to be purchased from the grid. Ideally, one could easily implement then, the biggest battery and therefore be able to supply at their loads any time, but in reality this is quite different, because it does not only depend on the amount of energy that it is produced by the PV panels but also economically speaking, bigger batteries mean bigger investments. And so before sizing the battery, the following factors should be taken into account:

- Number of autonomy days, i.e. the number of days that the system is able to run before recharging it.
- Amount of demanded power by the loads as well as the amount of generated power, although usually the PV panels should be sized bigger than the battery bank so that it compensates in case of power fluctuations, energy losses, etc.
- Money capital, or the amount of money the user is willing to spend on the PV system.

- Depth of discharge, although this parameter depends on the specific power needs and/or capacity, one should not forget that this parameter directly affects the battery's lifespan (as it is shown in Figure 5.7).

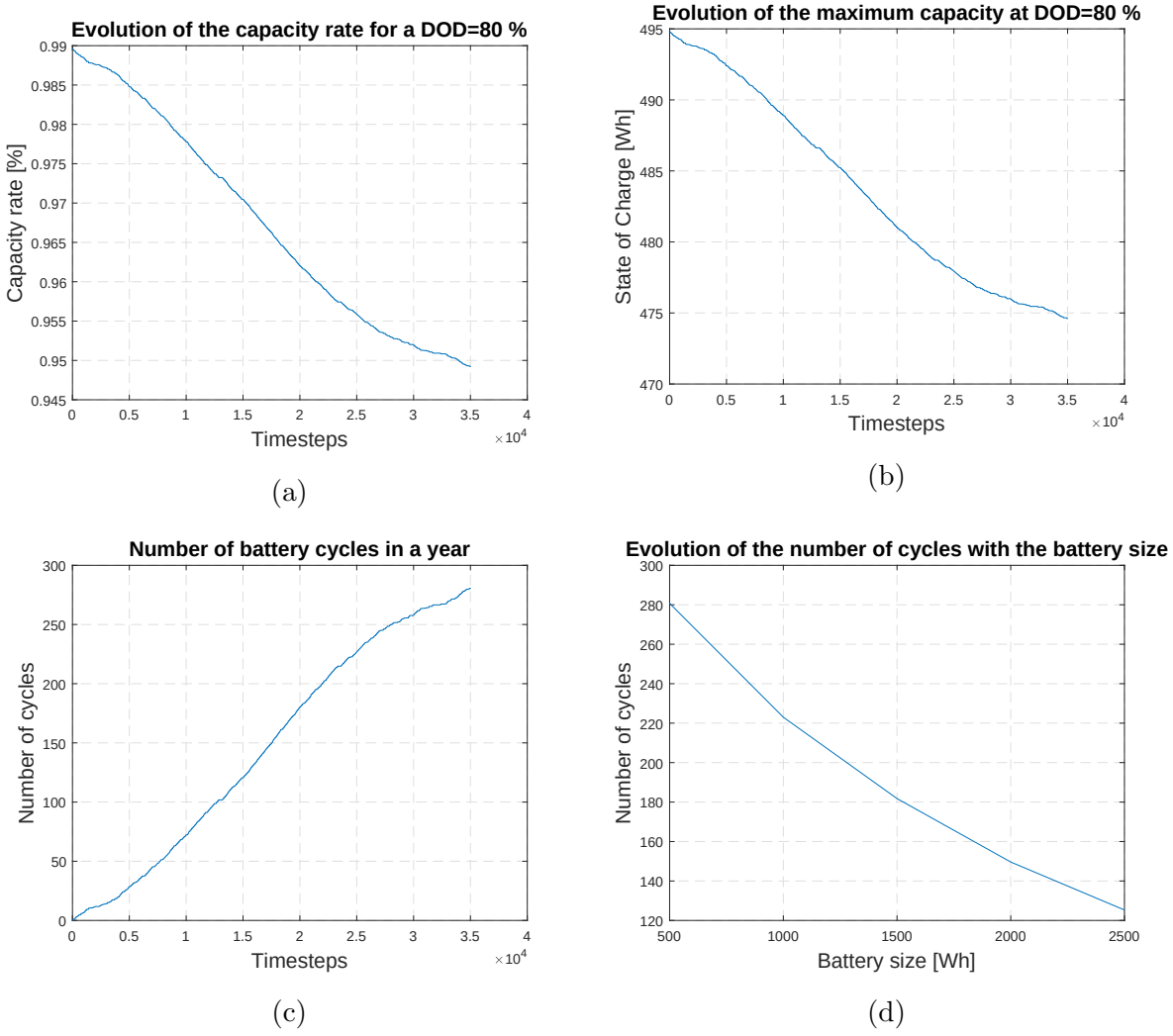

Figure 5.7.: Simulation results regarding the battery (a) Evolution of the capacity rate overtime for a DOD=80 % (b) Evolution of the SOC overtime for a DOD=80 % (c) Evolution of the number of cycles that the battery experiences during a year (d) Influence of the battery size over the number of cycles.

5.3. Overall results

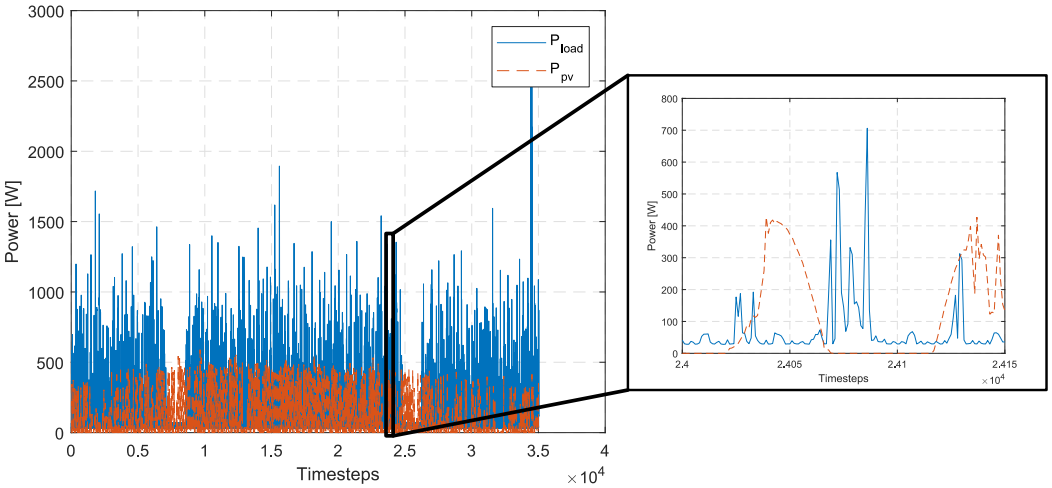

Figure 5.8.: Comparison between the produced power by the PV modules and the required power by the loads, simulated using the standard parameters.

As it is depicted in Figure 5.8, the amount of required power by the loads cannot be only covered with the generated power by the PV system, and so the grid plays its role as a power backup in order to fully supply the demand (c.f. Figure 5.9).

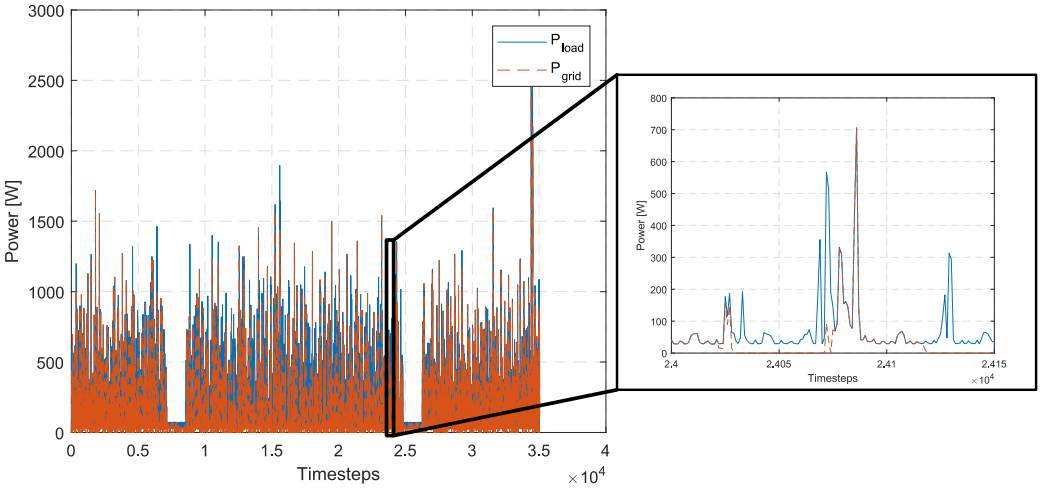

Figure 5.9.: Comparison between the required power by the loads and the needed energy from the grid, simulated using the standard parameters.

Finally, an interesting parameter that was suggested to be calculated was the SCR (Self-consumption Rate) and based on it, the DSS (Degree of Self-sufficiency) can be found. The first term indicates the amount of generated energy from the PV that is consumed or used to charge the battery. The second term is an indicator that describes the share of energy consumption that is covered by the power generated from the PV panels, when the DSS increases the amount of energy taken from the grid decreases [62]. The DSS is calculated as it follows [63]

$$DSS = \frac{SCR}{E_{\text{load}}} = \frac{\int \min(P_{\text{PV}}, P_{\text{load}}) \cdot dt}{E_{\text{load}}} \,. \tag{5.6}$$

Table 5.1.: Highlight of the results obtained after simulation over a period of a year.

Parameter	Value
E_{load} [kW h]	906.98
E_{PV} [kW h]	601.41
Degree of Self-Sufficiency (DSS) [%]	22.91

For the modeled and simulated system the obtained DDS is approximately 23%, which means that 23 % of the energy needed to feed the loads is supplied by the PV generator.

6. Discussion

The work presented a new concept of a photovoltaic system configuration, said system consists of a combination of a traditional stand-alone and a grid-connected system, i.e. the developed systems uses the same components as a stand-alone system, but it has a point of connection with the electric grid. But unlike grid-connected systems, the presented system only has a one-way connection, meaning that energy can only be injected from the grid to the system (and not the other way around, due to the country's regulations), therefore the grid's purpose is to merely supply energy when neither the PV generator nor the battery have enough energy. Evidently, in this system all the system's surplus is lost, due the aforementioned reason.

The PV system has been developed and constructed using some assumptions, for example values like temperature coefficients, series and parallel resistances have been obtained from existing literature. These assumption have been made due to the lack of data provided by the start-up company. Further research and relevant tests regarding this data could improve the system's accuracy. Another used assumption, was to consider an average value of the load's data that was measured in a three phase system, this was done because the start-up company utilizes smart meters that constantly detect the load in one phase, i.e. measuring the average load in one phase and therefore making the system simpler and more dynamical.

The model has some limitations, for example the battery's aging model does not consider temperature effects and it is known that temperature has a significant impact on the performance, safety, and cycle lifetime of LIB. Another limitation in the aging model is that it only allows a medium range of cycles (it works without problems up to 2000 cycles). Some other limitations are the fact that energy surplus cannot be injected into the grid (as it was mentioned) and that only one control strategy was able to be implemented in the system, in case that other types of control strategies are implemented, the first need to go through some necessary changes like including perfect prognosis.

7. Conclusion and outlook

In the present work, a domestic PV system with energy storage has been developed. More specifically, a Simulink model based on the series and parallel resistances model has been constructed. The input parameters, depend mainly on datasheet parameters and/or literature as well as temperature and irradiance. The last two parameters, are obtained from the Perez model, a sophisticated model that calculates the incident irradiance on a tilted plane, based on measured data obtained from the Meteorology and Geodynamics Central Institute. Additionally, current-voltage and power-voltage characteristics curves are plotted and the effects of temperature and irradiance have been demonstrated. It is concluded that higher irradiances and smaller temperatures are the best combination to achieve higher yields of power. Along the development of the PV model, some speed issues were detected due to handling big amounts of data and the long timeline considered. For this reason, mathematical equations were extracted from the results obtained from the PV Simulink model. It was also possible to implement the MPP, so that at all times the maximum power is obtained and its corresponding voltage and current. The PV model enables easily modifiable characteristic parameters, such as the short circuit current, open source voltage and PV cell technology, among others.

The model of the battery is done by means of power and energy balances, and implements four operational modes that depend on the load needs and the amount of stored energy and/or produced energy. Depending on that balance, the grid may or may not supply the remaining energy. However, at no point in time there is energy injection into the grid. A control strategy, based on the greedy operation was implemented as well as a degradation model, that incorporates the aging effects that a battery suffers along its lifespan due to the stress factors like charging/discharging cycles and depth of discharge directly affecting the battery's capacity and state of charge.

Modeling the inverter was performed by means of curve fitting, based on real measured data provided by a start-up company located in Graz, that was later on used to construct

the typical efficiency curve of an inverter. The aforementioned data helped to obtain two mathematical equations, one referred to the input power and the other referred to the output power of the inverter; both equations are able to work with any inverter size.

Once having all the components modeled, they were integrated into one single script, that is able to simulate a whole year of data reasonably fast and at the end calculates the amount of energy that is needed from the grid as well as a very important parameter in PV systems: the Degree of Self-sufficiency, which resulted in approximately 23 %, a reasonably fair result for a domestic PV system.

Lastly, a sensitivity analysis was carried out in order to find out how much of an impact some independent variables (like inclination angles, orientation, battery and inverter sizes, etc.) have on a dependent variable like the energy that is saved. Looking at the obtained results, it is possible to conclude that having a surface orientation between $-40°$ to $40°$ with an inclination between $10°$ to $50°$ (note than in PV panels vertically mounted[1], the energy savings can be significantly increased when changing the inclination to approximately $70°$), with a bigger area of incidence as well as big inverter and battery sizes would result in bigger yields of energy saved. However as it was discussed in Chapter 5, these last three parameters are subjected to economical and technical limitations as well as to the load demand and PV production. Therefore, a compromise between these limitations has to be made by the user made based on the results from this model that aimed to develop a tool that helps to determine the best configuration be.

Future work will focus on improving the system's accuracy, by means of using real temperature coefficients and series and parallel resistances rather than taking them from literature. Furthermore, depth of discharge curves with higher number of cycles should be investigated and temperature effects should also be implemented in the aging model of the battery model and more control strategies should be implemented, i.e. based on the literature review that was carried out the empirical part can be included in the presented model.

[1] $\beta = 90°$

Bibliography

[1] European Comission, "2020 climate & energy package," accessed: 2018-03-27. [Online]. Available: https://ec.europa.eu/clima/policies/strategies/2020_en

[2] ——, "2030 climate & energy framework," accessed: 2018-03-27. [Online]. Available: https://ec.europa.eu/clima/policies/strategies/2030_en

[3] B. Sørensen, *Solar Energy Storage*. Elsevier Science, 2015. [Online]. Available: https://books.google.at/books?id=Qs-cBAAAQBAJ

[4] Renewable Energy Policy Network for the 21st Century, "Renewables 2017 Global Status Report," International Energy Agency, Tech. Rep., 2017.

[5] International Energy Agency, "Technology Roadmap Solar photovoltaic energy," In *International Energy Agency*, pp. 1–42, 2010.

[6] European Comission, "Energy efficiency in buildings." [Online]. Available: https://ec.europa.eu/energy/en/topics/energy-efficiency/buildings

[7] T. M. Letcher, *Storing Energy: with Special Reference to Renewable Energy Sources*. Elsevier Science, 2016. [Online]. Available: https://books.google.at/books?id=TPReBwAAQBAJ

[8] E-Control, "Technische und organisatorische Regeln für Betreiber und Benutzer von Netzen," 7 2016. [Online]. Available: https://www.e-control.at/documents/20903/388512/TOR_D4_V2.3+ab+1.7.2016.pdf/1fbc3aff-36a6-4eee-8de5-6027eaa53a89

[9] R. Messenger and A. Abtahi, *Photovoltaic Systems Engineering*. CRC Press, 2017. [Online]. Available: https://books.google.at/books?id=C3BGDgAAQBAJ

[10] M. Boxwell, *Solar Electricity Handbook: A Simple, Practical Guide to Solar Energy - Designing and Installing Photovoltaic Solar Electric Systems*. Greenstream Publishing.

[11] B. Zhao, C. Wang, and X. Zhang, *Grid-Integrated and Standalone Photovoltaic Distributed Generation Systems: Analysis, Design, and Control*. Wiley, 2017. [Online]. Available: https://books.google.at/books?id=yNk5DwAAQBAJ

[12] Franz Kininger-Rationelle Energiewandlung, "Photovoltaic Systems Technology," Universitaät Kassel.

[13] European Comission, "Photovoltaic Solar Energy: Development and current research," Tech. Rep., 2009.

[14] E. Lorenzo, *Electricidad solar: ingenieria de los sistemas fotovoltaicos*. Progensa: Promotora General de Estudios, 1994.

[15] S. A. Kalagirou, *Solar Energy Engineering: Processes and Systems*. Academic Press, 2013.

[16] C. S. Solanki, *Solar Photovoltaics: Fundamentals, Technologies And Applications*. PHI Learning, 2015. [Online]. Available: https://books.google.at/books?id=y1W2CAAAQBAJ

[17] Fraunhofer Institute for Solar Energy Systems, "Photovoltaics report," Fraunhofer ISE, Tech. Rep., 2018. [Online]. Available: www.ise.fraunhofer.de

[18] H. Bellia, R. Youcef, and M. Fatima, "A detailed modeling of photovoltaic module using MATLAB," In *NRIAG Journal of Astronomy and Geophysics*, Vol. 3, No. 1, pp. 53 – 61, 2014. [Online]. Available: http://www.sciencedirect.com/science/article/pii/S2090997714000182

[19] M. G. Villalva, J. R. Gazoli, and E. R. Filho, "Comprehensive Approach to Modeling and Simulation of Photovoltaic Arrays," In *IEEE Transactions on Power Electronics*, Vol. 24, No. 5, pp. 1198–1208, May 2009.

[20] H. B. Vika, "Modelling of Photovoltaic Modules with Battery Energy Storage in Simulink/Matlab," Master's thesis, Norwegian University of Science and Technology Trondheim, 2014.

[21] H.-l. Tsai, C.-s. Tu, and Y.-j. Su, "Development of Generalized Photovoltaic Model Using MATLAB / SIMULINK," In *Proceedings of the World Congress on Engineering and Computer Science 2008 WCECS 2008, October 22 - 24, 2008, San Francisco, USA*, p. 6, 2008.

[22] J. A. Duffie and W. A. Beckman, *Solar Engineering of Thermal Processes: Fourth Edition*, 2013.

[23] Viorel Badescu, *Modeling Solar Radiation at the Earth's Surface: Recent Advances*. Springer Science & Business Media, 2008.

[24] P. Jain, "Modelling of the diffuse radiation in environment conscious architecture: The problem and its management," Vol. 6, No. 4, pp. 493–500, 1989.

[25] US Department of Energy., "Sky Radiance Model." [Online]. Available: https://bigladdersoftware.com/epx/docs/8-0/engineering-reference/page-033.html

[26] C. Honsberg and S. Bowden, "Photovoltaic Education network," accessed: 2018-07-18. [Online]. Available: https://pveducation.org/

[27] ENDESA and Real Academia de Ingeniería, *El almacenamiento de energía en la distribución elćtrica del futuro*. Grafilia S.L., 2017.

[28] O. Moraes-Toledo, D. Oliveira-Filho, and A. S. A. Cardoso-Diniz, "Distributed photovoltaic generation and energy storage systems: A review," In *Renewable and Sustainable Energy Reviews*, Vol. 14, No. 1, pp. 506 – 511, 2010. [Online]. Available: http://www.sciencedirect.com/science/article/pii/S136403210900207X

[29] A. Chaurey and S. Deambi, "Battery storage for PV power systems: An overview," In *Renewable Energy*, Vol. 2, No. 3, pp. 227 – 235, 1992. [Online]. Available: http://www.sciencedirect.com/science/article/pii/0960148192900363

[30] A. Jossen, J. Garche, and D. Sauer, "Operation conditions of batteries in PV applications," Vol. 76, pp. 759–769, 06 2004.

[31] F. Díaz-González, "Energy storage systems for power networks," 2017, UPC's course material for the Energy Storage lectures, retrieved from www.http://atenea.upc.edu.

[32] MIT Electric Vehicle Team, "A guide to understanding battery specifications." [Online]. Available: http://web.mit.edu/evt/summary_battery_specifications.pdf

[33] Solar365: the home to alternative energy, "Deep Cycle Batteries and Discharge." [Online]. Available: http://www.solar365.com/solar/photovoltaic/deep-cycle-batteries-discharge

[34] GWL Power, "Lithium and solar power LiFePO4." [Online]. Available: http://gwl-power.tumblr.com/post/26696964746/depth-of-discharge-dod-all-battery

[35] S. Santhanagopalan, K. Smith, J. Neubauer, G. Kim, A. Pesaran, and M. Keyser, *Design and Analysis of Large Lithium-Ion Battery Systems*, ser. Artech House power engineering series. Artech House Publishers, 2014. [Online]. Available: https://books.google.at/books?id=8PfmBgAAQBAJ

[36] J. Jung, L. Zhang, and J. Zhang, *Lead-Acid Battery Technologies: Fundamentals, Materials, and Applications*, ser. Electrochemical Energy Storage and Conversion. CRC Press, 2015. [Online]. Available: https://books.google.at/books?id=I_cOCgAAQBAJ

[37] J. Zhang, L. Zhang, H. Liu, A. Sun, and R. Liu, *Electrochemical Technologies for Energy Storage and Conversion.* Wiley, 2012. [Online]. Available: https://books.google.at/books?id=AN3B3L5RtqUC

[38] L. Hewitson, M. Brown, B. Ramesh, and R. Balakrishnan, *Practical Power System Protection*, ser. Electronics & Electrical. Newnes, 2005. [Online]. Available: https://books.google.at/books?id=SSSFt-58uMAC

[39] H. D. Abruña, Y. Kiya, and J. C. Henderson, "Batteries and electrochemicanl capacitors," In *Physics Today*, 2008.

[40] A. Saengprajak, *Efficiency of Demand Side Management Measures in Small Village Electrification Systems.* Kassel University Press GmbH, 2007. [Online]. Available: https://books.google.at/books?id=PPWgT-_gFC4C

[41] F. Luo and H. Ye, *Advanced DC/AC Inverters: Applications in Renewable Energy*, ser. Power Electronics, Electrical Engineering, Energy, and Nanotechnology. CRC Press, 2017. [Online]. Available: https://books.google.at/books?id=NJkuDwAAQBAJ

[42] S. Sumathi, L. Kumar, and P. Surekha, *Solar PV and Wind Energy Conversion Systems: An Introduction to Theory, Modeling with MATLAB/SIMULINK, and the Role of Soft Computing Techniques*, ser. Green Energy and Technology. Springer International Publishing, 2015. [Online]. Available: https://books.google.at/books?id=tl72BwAAQBAJ

[43] International Renewable Energy Agency, "Renewable power generation costs in 2017," Tech. Rep., 2018.

[44] H. Choi, W. Zhao, M. Ciobotaru, and V. G. Agelidis, "Large-scale PV system based on the multiphase isolated DC/DC converter," pp. 801–807, June 2012.

[45] S. Ozdemir, N. Altin, and I. Sefa, "Single stage three level grid interactive MPPT inverter for PV systems," In *Energy Conversion and Management*, Vol. 80, pp. 561 – 572, 2014. [Online]. Available: http://www.sciencedirect.com/science/article/pii/S0196890414000934

[46] PennState Department of Energy and Mineral Engineering, "AE 868: Commercial Solar Electric Systems - Inverter types and classification," accessed: 2018-07-18. [Online]. Available: https://www.e-education.psu.edu/ae868/node/904

[47] Electronic Design, "Do not judge solar PV system's efficacy by inverter efficiency alone," accessed: 2018-07-18. [Online]. Available: https://www.e-education.psu.edu/ae868/node/904

[48] A. Cabrera-Tobar, E. Bullich-Massagué, M. Aragües-Peñalba, and O. Gomis-Bellmunt, "Topologies for large scale photovoltaic power plants," In *Renewable and Sustainable Energy Reviews*, 2016.

[49] K. Mertens, *Photovoltaics: Fundamentals, Technology and Practice*, ser. Wiley Desktop Editions Series. Wiley, 2014.

[50] B. Burger and D. Kranzer, "Extreme high efficiency PV-power converters," In *2009 13th European Conference on Power Electronics and Applications*, pp. 1–13, 2009, Barcelona.

[51] J. Moshövel Struth, K.-P. Kairies, M. Leuthold, A. Aretz, M. Bost, S. Gährs, M. Cramer, E. Szczechowicz, B. Hirschl, A. Schnettler, and D. Sauer, "PV-Benefit: A Critical Review of the Effect of Grid Integrated PV-Storage-Systems," 11 2013.

[52] M. Pietsch, *Optimierung eines Photovoltaikspeichers. Vergleich diverser Operationsstrategien zur Kostenminimierung.* Diplomica Verlag, 2016. [Online]. Available: https://books.google.at/books?id=A-JrDAAAQBAJ

[53] L. Bird, J. Cochran, and X. Wang, "Wind and Solar Energy Curtailment: Experience and Practices in the United States," National Renewable Energy Laboratory, Tech. Rep., 2014.

[54] R. Golden and B. Paulos, "Curtailment of Renewable Energy in California and

Beyond," In *The Electricity Journal*, Vol. 28, No. 6, pp. 36 – 50, 2015. [Online]. Available: http://www.sciencedirect.com/science/article/pii/S1040619015001372

[55] P. Pretschuh, "Solares Energiepotential kleiner und mittlerer Städte," Montanuniversität Leoben, 2016.

[56] M. Freunek, M. Freunek, and L. M. Reindl, "Maximum efficiencies of indoor photovoltaic devices," In *IEEE Journal of Photovoltaics*, Vol. 3, No. 1, pp. 59–64, Jan 2013.

[57] M. Hatti, *Artificial Intelligence in Renewable Energetic Systems: Smart Sustainable Energy Systems*, ser. Lecture Notes in Networks and Systems. Springer International Publishing, 2018. [Online]. Available: https://books.google.at/books?id=ufxQDwAAQBAJ

[58] R. Spotnitz, "Simulation of capacity fade in lithium-ion batteries," In *Journall of Power Sources*, Vol. 113, No. 1, pp. 72 – 80, 2003. [Online]. Available: http://www.sciencedirect.com/science/article/pii/S0378775302004901

[59] B. Xu, A. Oudalov, A. Ulbig, G. Andersson, and D. S. Kirschen, "Modeling of Lithium-Ion Battery Degradation for Cell Life Assessment," In *IEEE Transactions on Smart Grid*, Vol. 9, No. 2, pp. 1131–1140, March 2018.

[60] Smart Battery, "Deep cycle lithium-ion battery," accessed: 2018-06-25. [Online]. Available: https://www.lithiumion-batteries.com/products/product/12v-100ah-lithium-ion-battery.php

[61] N. D. Pflugradt, "Modellierung von Wasser- und Energieverbräuchen in Haushalten," Ph.D. dissertation, Technischen Universität Chemnitz, 7 2016. [Online]. Available: https://tinyurl.com/yc7bwtlr

[62] J. Weniger, T. Tjaden, and V. Quaschning, "Sizing of Residential PV Battery Systems," In *Energy Procedia*, Vol. 46, pp. 78 – 87, 2014, 8th International Renewable Energy Storage Conference and Exhibition (IRES 2013). [Online]. Available: http://www.sciencedirect.com/science/article/pii/S1876610214001763

[63] W. Gawlik, "Degrees of self-sufficiencies," 2016.

Appendices

A. A deep dive into the battery's aging effects

In the following section, different curves and their corresponging curve-fitting equation, that were used and implemented in the aging model used in the battery, are going to be shown in detail.

A.1. Capacity rates vs number of cycles for a DOD=100% and a DOD=90%

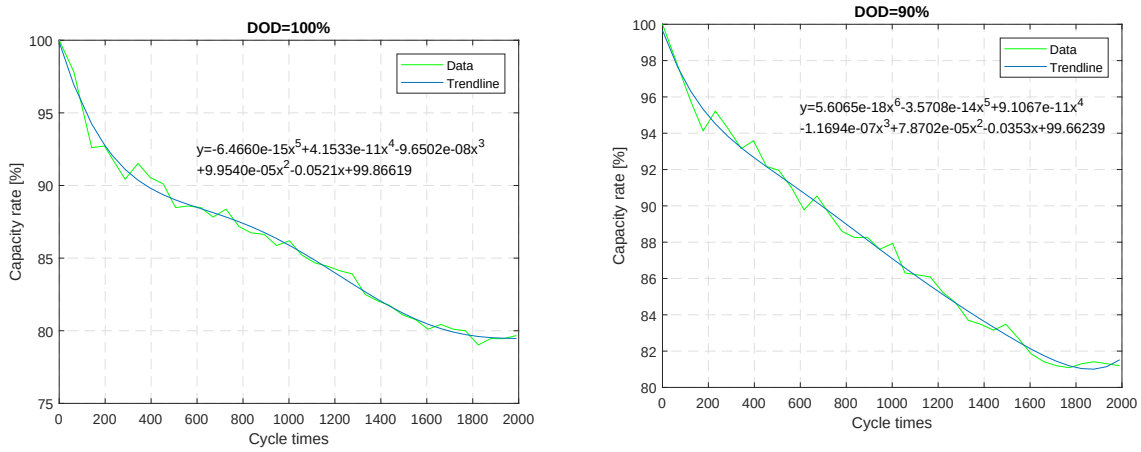

(a) (b)

Figure A.1.: Capacity rate vs number of cycles (a) For a DOD of 100% (b) for a DOD of 90%.

A.2. Capacity rates vs number of cycles for a DOD=80% and a DOD=70%

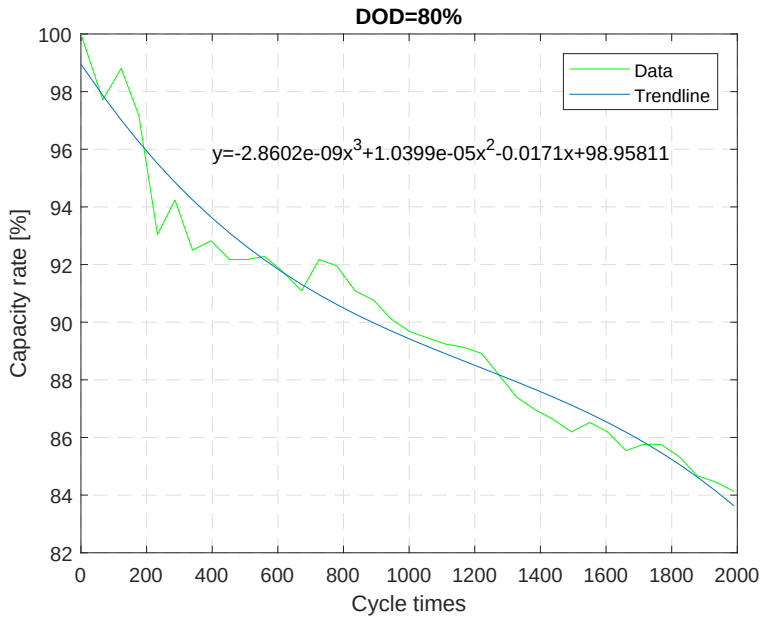

(a)

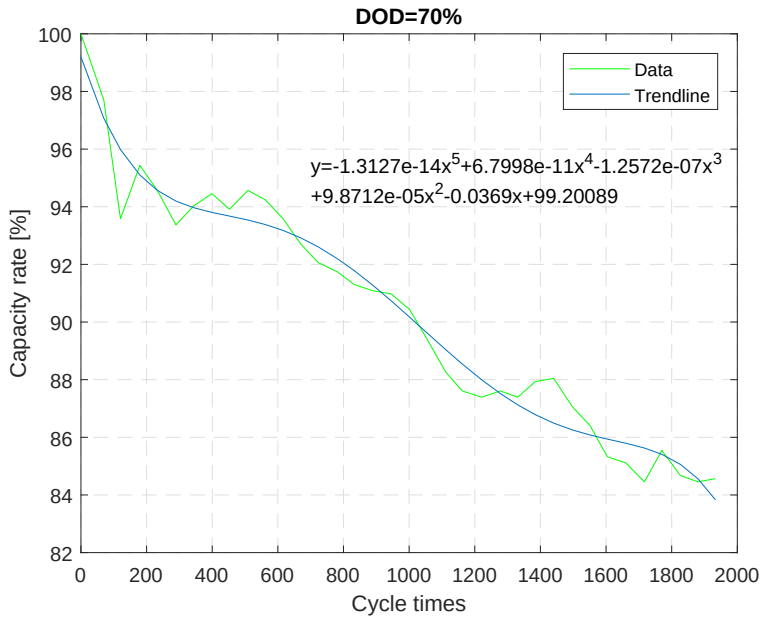

(b)

Figure A.2.: Capacity rate vs number of cycles (a) For a DOD of 80% (b) for a DOD of 70%.

A.3. Capacity rates vs number of cycles for a DOD=60% and a DOD=50%

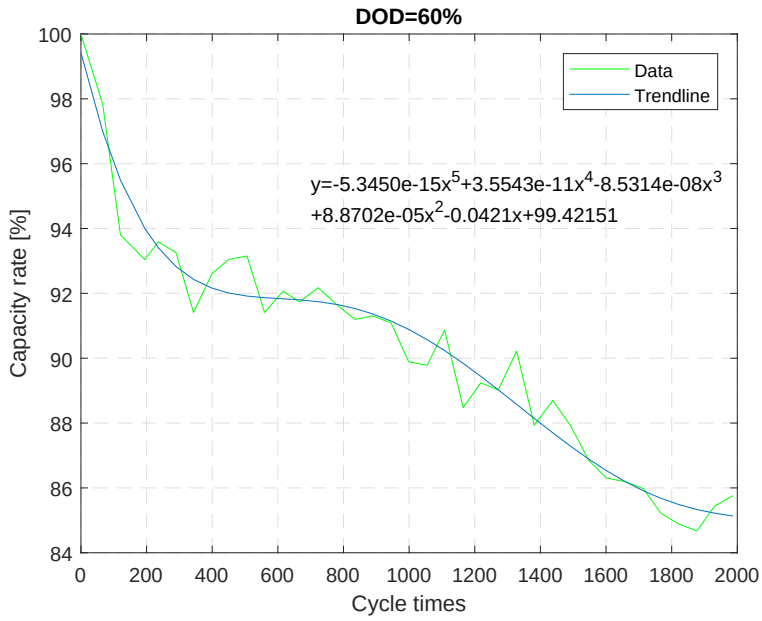

(a)

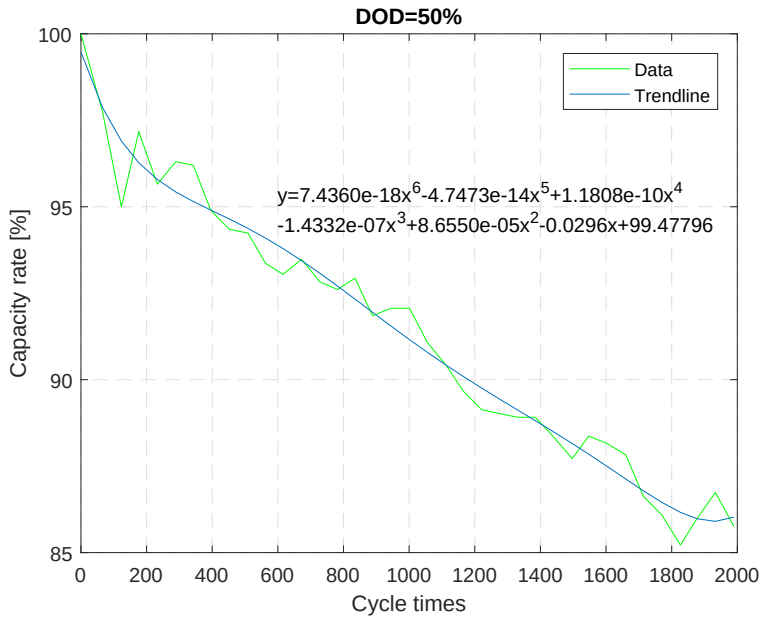

(b)

Figure A.3.: Capacity rate vs number of cycles (a) For a DOD of 60% (b) for a DOD of 50%.

A.4. Capacity rates vs number of cycles for a DOD=40% and a DOD=30%

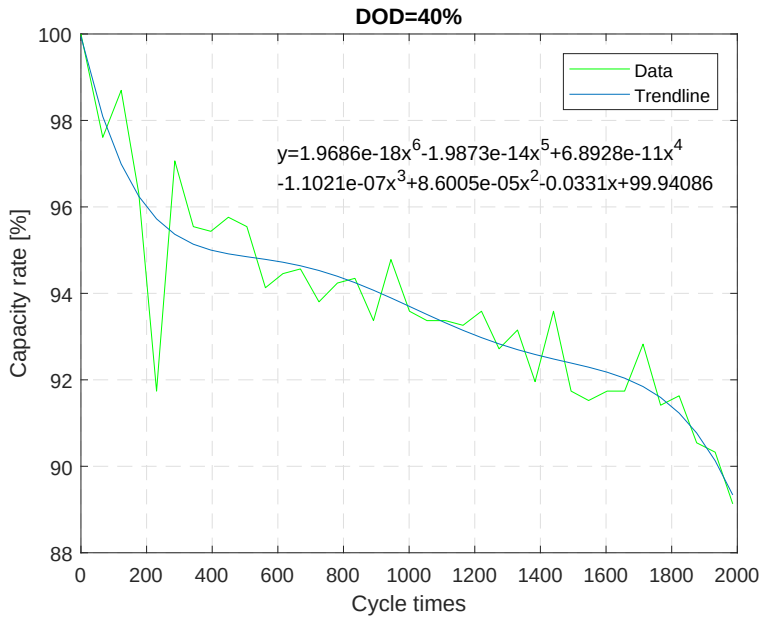

(a)

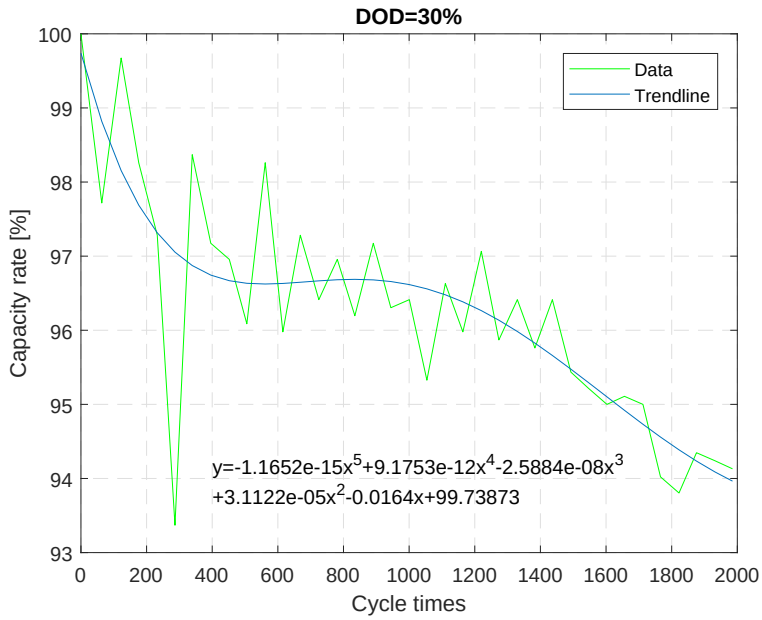

(b)

Figure A.4.: Capacity rate vs number of cycles (a) For a DOD of 40% (b) for a DOD of 30%.

A.5. Capacity rates vs number of cycles for a DOD=20% and a DOD=10%

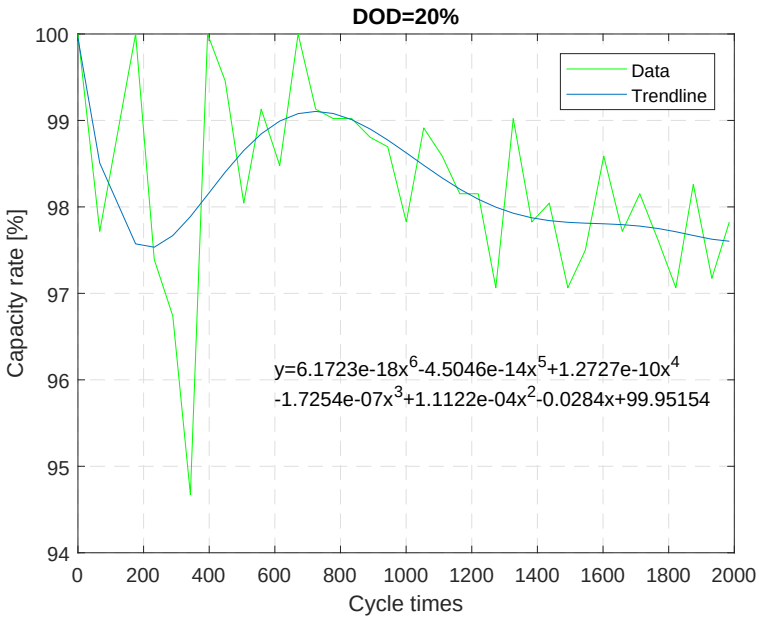

(a)

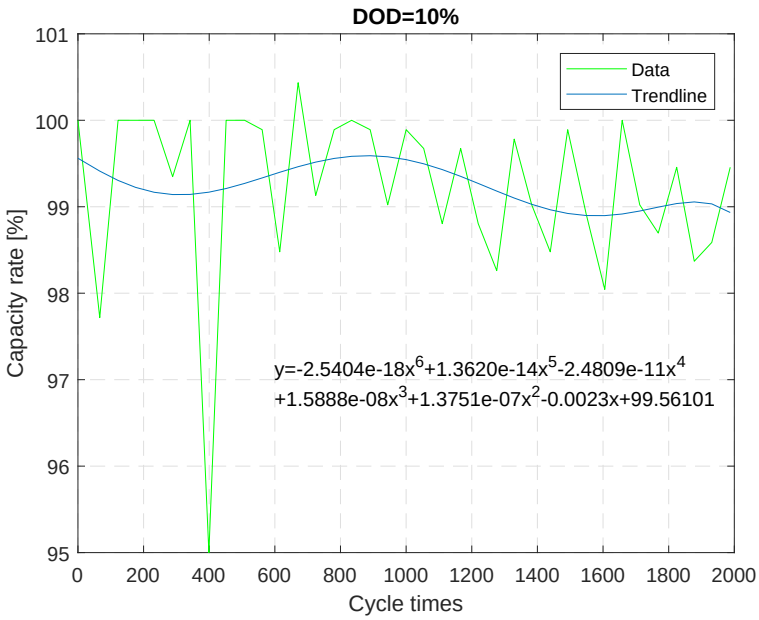

(b)

Figure A.5.: Capacity rate vs number of cycles (a) For a DOD of 20% (b) for a DOD of 10%.